Continuum Mechanics and Atomistic Modeling of Graphene

Rui Huang

Center for Mechanics of Solids, Structures and Materials
Department of Aerospace Engineering and Engineering Mechanics
The University of Texas at Austin

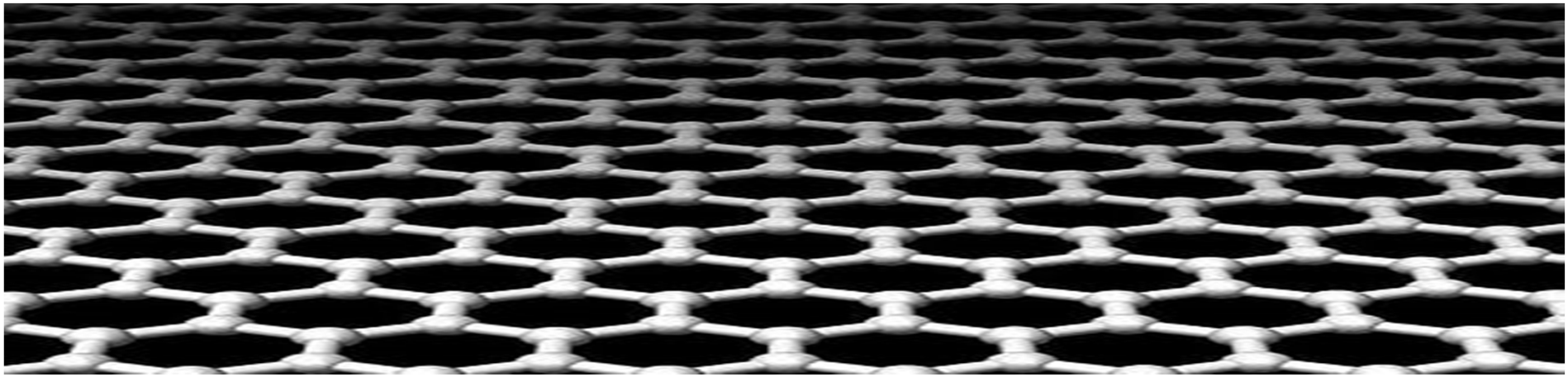

Acknowledgments

- **Qiang Lu** (postdoc)
- **Wei Gao** (graduate student)
- **Zachery Aitken** (undergraduate student, now at Caltech)
- Prof. Marino Arroyo (Spain)
- Prof. Li Shi (UT/ME)

- Funding: NSF (ARRA)

From Wikipedia:

Graphene is a one-atom-thick planar sheet of sp^2-bonded carbon atoms that are densely packed in a honeycomb crystal lattice. The term *Graphene* was coined as a combination of graphite and the suffix -ene by Hanns-Peter Boehm, who described single-layer carbon foils in 1962. Graphene is most easily visualized as an atomic-scale chicken wire made of carbon atoms and their bonds.

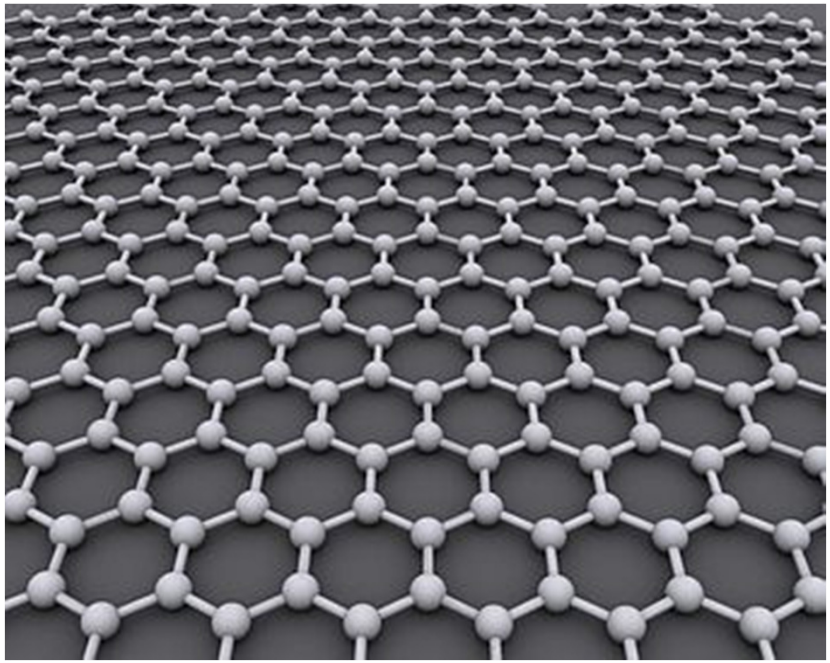

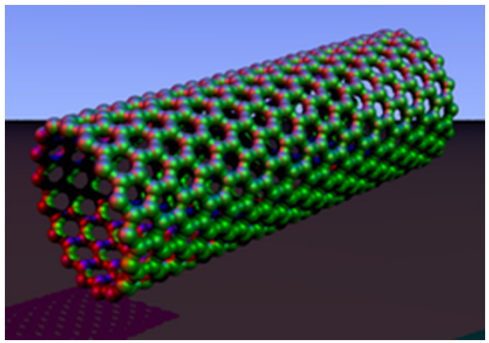

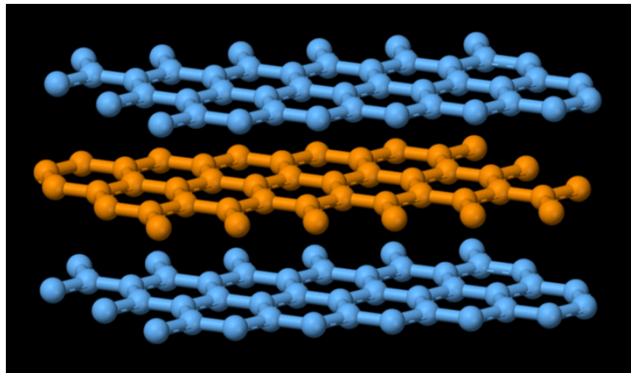

Graphene Based Devices

Patterned graphene on oxide for bipolar p-n-p junctions

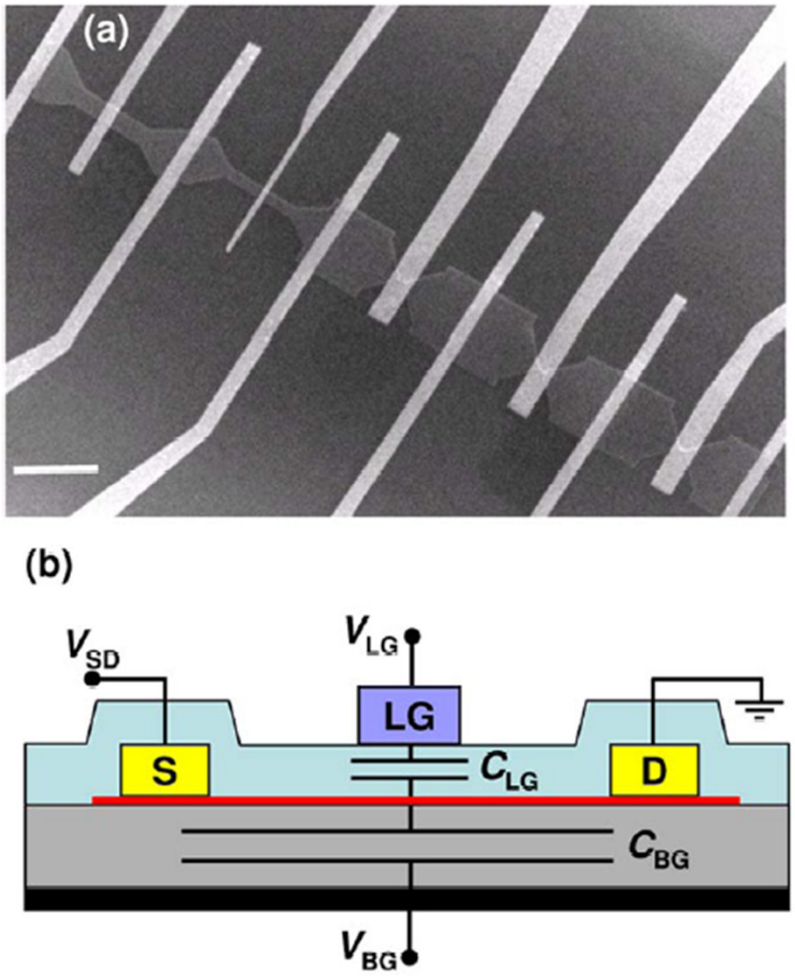

Ozyilmaz et al., 2007.

Suspended nanoribbons for NEMS devices

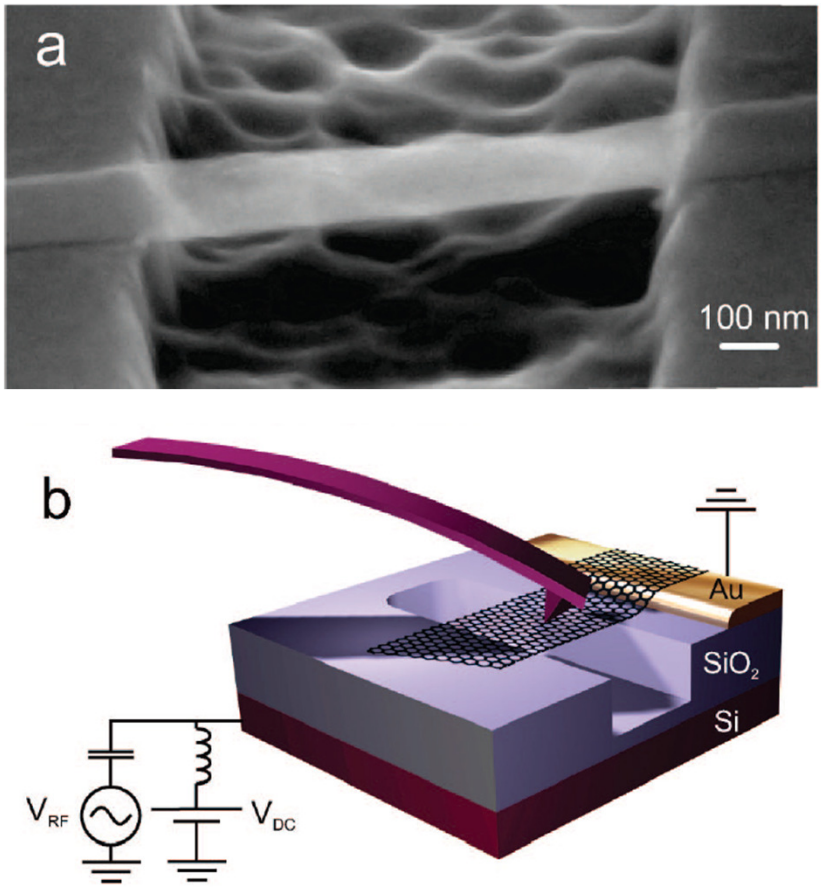

Garcia-Sanchez, et al., 2008.

Mechanical properties of monolayer graphene

- High in-plane stiffness (Young's modulus)
- High tensile strength
- High bending stiffness (relative to its own weight)

- Isotropic, linearly elastic under infinitesimal deformation
- Anisotropic, nonlinear under finite deformation

➢ *Graphene nanoribbons: edge effects?*

➢ *Substrate-supported graphene: adhesive interactions?*

Nonlinear Continuum Mechanics of 2D Sheets

2D-to-3D deformation gradient:

$$F_{iJ} = \frac{\partial x_i}{\partial X_J}$$

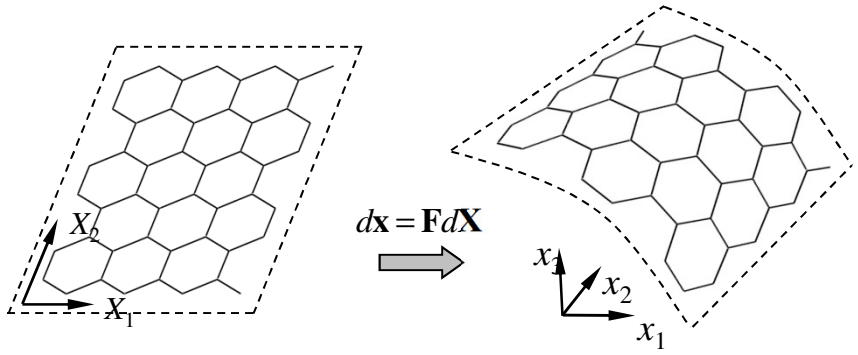

In-plane deformation: 2D Green-Lagrange strain tensor

$$E_{JK} = \frac{1}{2}\left(F_{iJ}F_{iK} - \delta_{JK}\right)$$

Bending: 2D curvature tensor (strain gradient)

$$\mathrm{K}_{IJ} = n_i \frac{\partial F_{iI}}{\partial X_J} = n_i \frac{\partial^2 x_i}{\partial X_I \partial X_J}$$

Strain energy (hyperelasticity):

$$U = \int_A \Phi\left(\mathbf{E}, \mathbf{K}\right) dA$$

Lu and Huang, Int. J. Applied Mechanics 1, 443-467 (2009).

2D Stresses and Moments

2nd Piola-Kirchoff stress and moment
(work conjugates)

$$S_{IJ} = \frac{\partial \Phi}{\partial E_{IJ}} \qquad M_{IJ} = \frac{\partial \Phi}{\partial \mathrm{K}_{IJ}}$$

Tangent moduli:

$$C_{IJKL} = \frac{\partial S_{IJ}}{\partial E_{KL}} = \frac{\partial^2 \Phi}{\partial E_{IJ} \partial E_{KL}} \qquad D_{IJKL} = \frac{\partial M_{IJ}}{\partial \mathrm{K}_{KL}} = \frac{\partial^2 \Phi}{\partial \mathrm{K}_{IJ} \partial \mathrm{K}_{KL}}$$

$$\Lambda_{IJKL} = \frac{\partial S_{IJ}}{\partial \mathrm{K}_{KL}} = \frac{\partial M_{KL}}{\partial E_{IJ}} = \frac{\partial^2 \Phi}{\partial E_{IJ} \partial \mathrm{K}_{KL}}$$

Intrinsic coupling between tension and bending

An incremental form of the generally nonlinear and anisotropic behavior:

$$\begin{pmatrix} dS_{11} \\ dS_{22} \\ dS_{12} \end{pmatrix} = \begin{bmatrix} C_{11} & C_{12} & C_{13} \\ C_{21} & C_{22} & C_{23} \\ C_{31} & C_{32} & C_{33} \end{bmatrix} \begin{pmatrix} dE_{11} \\ dE_{22} \\ 2dE_{12} \end{pmatrix} + \begin{bmatrix} \Lambda_{11} & \Lambda_{12} & \Lambda_{13} \\ \Lambda_{21} & \Lambda_{22} & \Lambda_{23} \\ \Lambda_{31} & \Lambda_{32} & \Lambda_{33} \end{bmatrix} \begin{pmatrix} d\mathrm{K}_{11} \\ d\mathrm{K}_{22} \\ 2d\mathrm{K}_{12} \end{pmatrix}$$

$$\begin{pmatrix} dM_{11} \\ dM_{22} \\ dM_{12} \end{pmatrix} = \begin{bmatrix} D_{11} & D_{12} & D_{13} \\ D_{21} & D_{22} & D_{23} \\ D_{31} & D_{32} & D_{33} \end{bmatrix} \begin{pmatrix} d\mathrm{K}_{11} \\ d\mathrm{K}_{22} \\ 2d\mathrm{K}_{12} \end{pmatrix} + \begin{bmatrix} \Lambda_{11} & \Lambda_{21} & \Lambda_{31} \\ \Lambda_{12} & \Lambda_{22} & \Lambda_{32} \\ \Lambda_{13} & \Lambda_{23} & \Lambda_{33} \end{bmatrix} \begin{pmatrix} dE_{11} \\ dE_{22} \\ 2dE_{12} \end{pmatrix}$$

Lu and Huang, Int. J. Applied Mechanics 1, 443-467 (2009).

Units for 2D quantities

$\Phi(\mathbf{E},\mathbf{K})$ strain energy density function: J/m^2

$S_{IJ} = \dfrac{\partial \Phi}{\partial E_{IJ}}$ 2D stress: N/m

$C_{IJKL} = \dfrac{\partial S_{IJ}}{\partial E_{KL}} = \dfrac{\partial^2 \Phi}{\partial E_{IJ}\partial E_{KL}}$ 2D in-plane modulus: N/m

$M_{IJ} = \dfrac{\partial \Phi}{\partial \mathrm{K}_{IJ}}$ moment intensity: (N-m)/m

$D_{IJKL} = \dfrac{\partial M_{IJ}}{\partial \mathrm{K}_{KL}} = \dfrac{\partial^2 \Phi}{\partial \mathrm{K}_{IJ}\partial \mathrm{K}_{KL}}$ bending modulus: N-m

$\Lambda_{IJKL} = \dfrac{\partial S_{IJ}}{\partial \mathrm{K}_{KL}} = \dfrac{\partial M_{KL}}{\partial E_{IJ}} = \dfrac{\partial^2 \Phi}{\partial E_{IJ}\partial \mathrm{K}_{KL}}$ coupling modulus: N

➢ Analogous to the 2D plate/shell theories (but no thickness).

Atomistic Modeling of Graphene

- 2nd-generation REBO potential (Brenner et al., 2002)
  - Bond angle effect (second-nearest neighbors)
  - Dihedral angle effect (third-nearest neighbors)
  - Radical energetics (defects and edges)

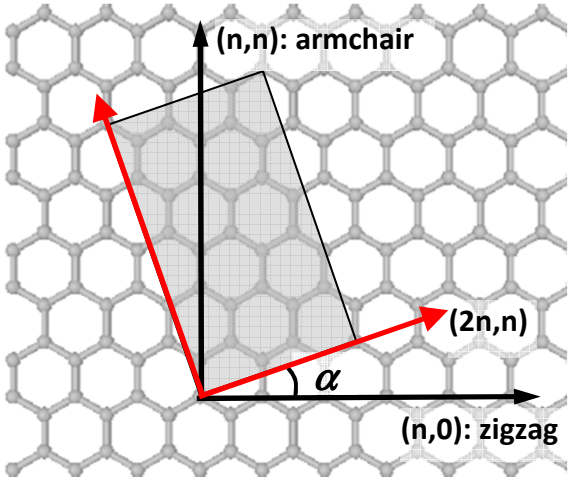

- Molecular Mechanics: energy minimization for static equilibrium states.

- Stress and moment calculations
  - Energy derivation
  - Virial stress calculations
  - Direct force evaluation

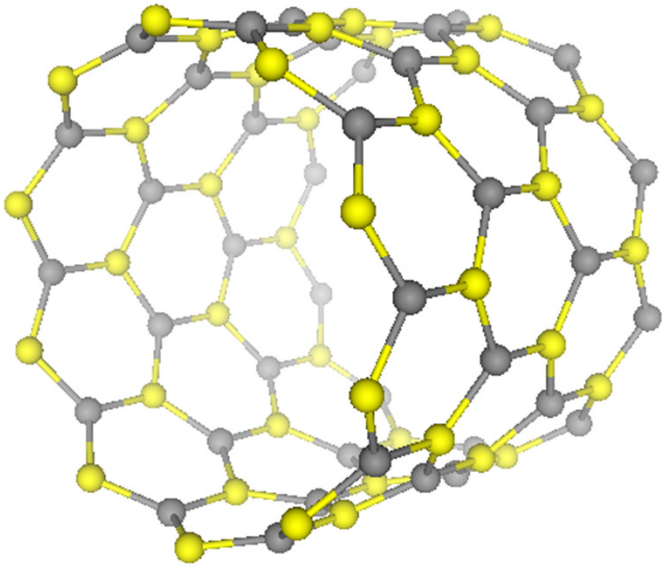

Uniaxial Stretch of Monolayer Graphene

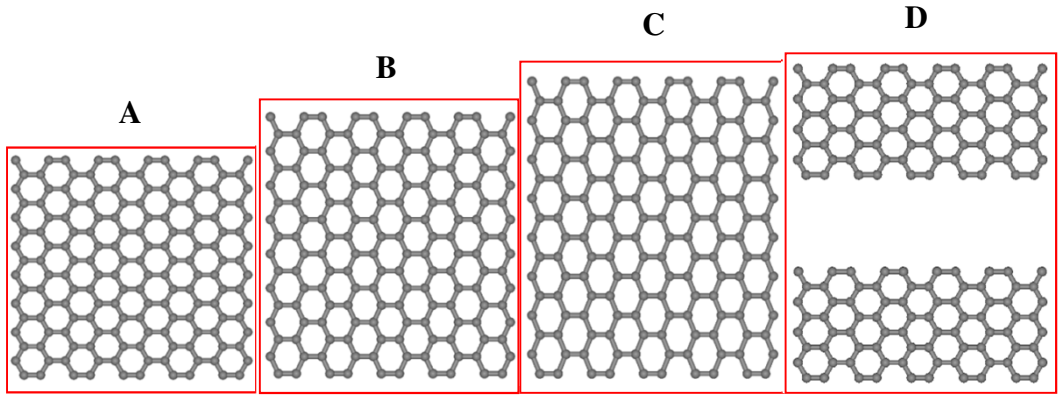

Nominal stress-strain relation:

$$P_{11}(\varepsilon) = \frac{d\Phi}{d\varepsilon}$$

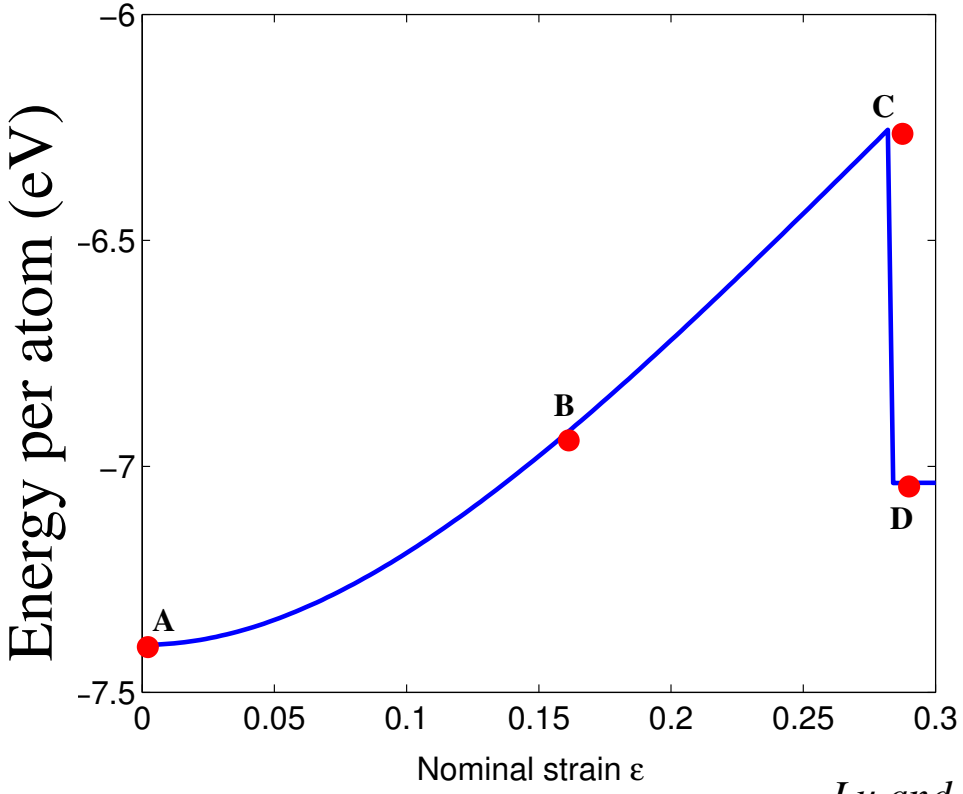

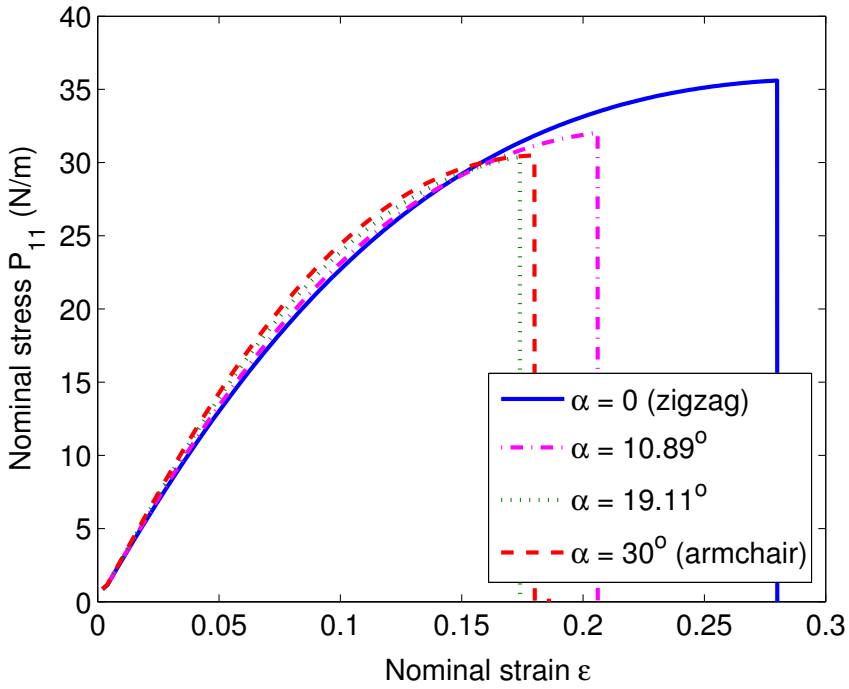

Lu and Huang, Int. J. Applied Mechanics 1, 443-467 (2009).

Anisotropic tangent moduli

$$\begin{pmatrix} dS_{11} \\ dS_{22} \\ dS_{12} \end{pmatrix} = \begin{pmatrix} C_{11} & C_{12} & C_{13} \\ C_{21} & C_{22} & C_{23} \\ C_{31} & C_{32} & C_{33} \end{pmatrix} \begin{pmatrix} dE_{11} \\ dE_{22} \\ 2dE_{12} \end{pmatrix}$$

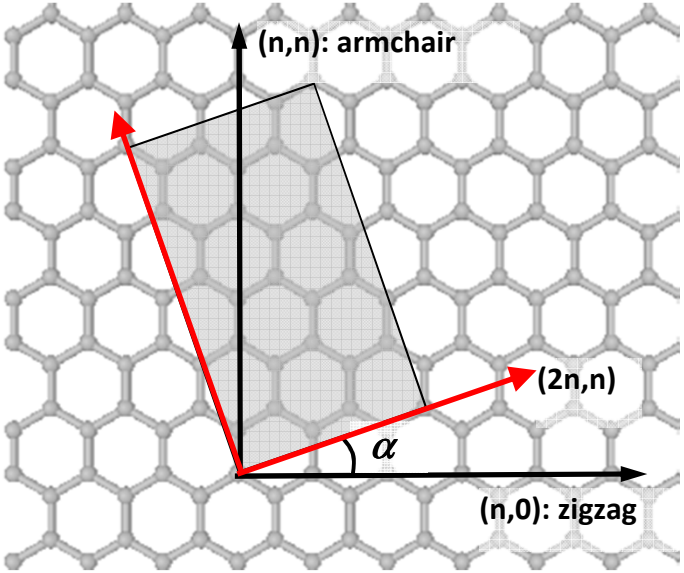

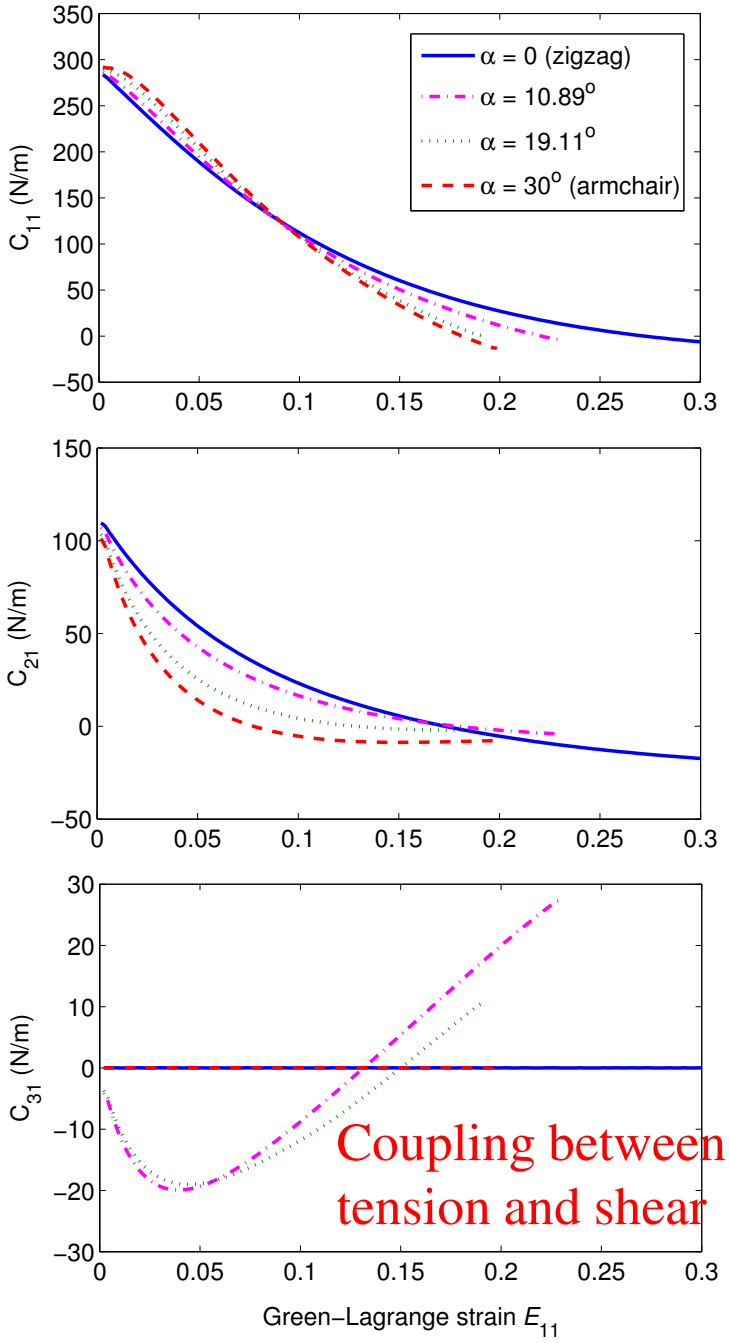

Graphene is linear and isotropic under infinitesimal deformation, but becomes nonlinear and anisotropic under finite deformation.

Lu and Huang, Int. J. Applied Mechanics 1, 443-467 (2009).

Fracture strength under uniaxial stretch

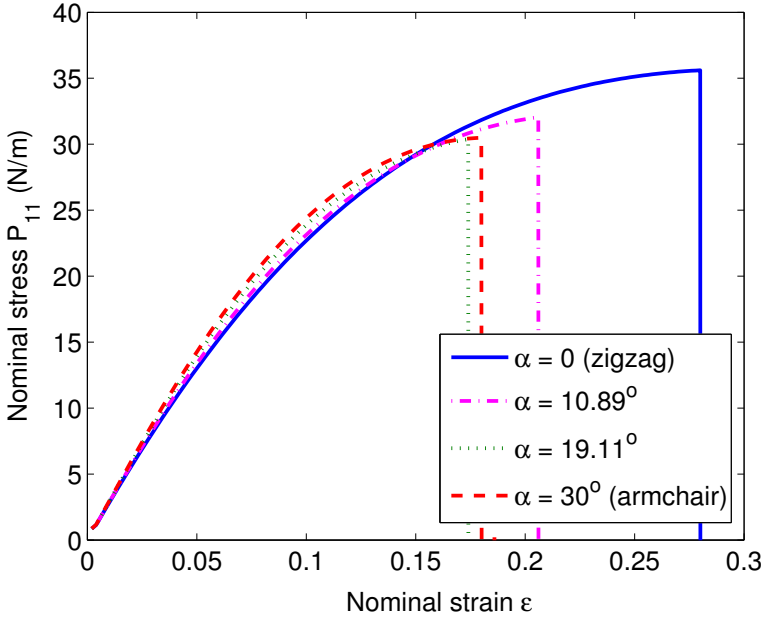

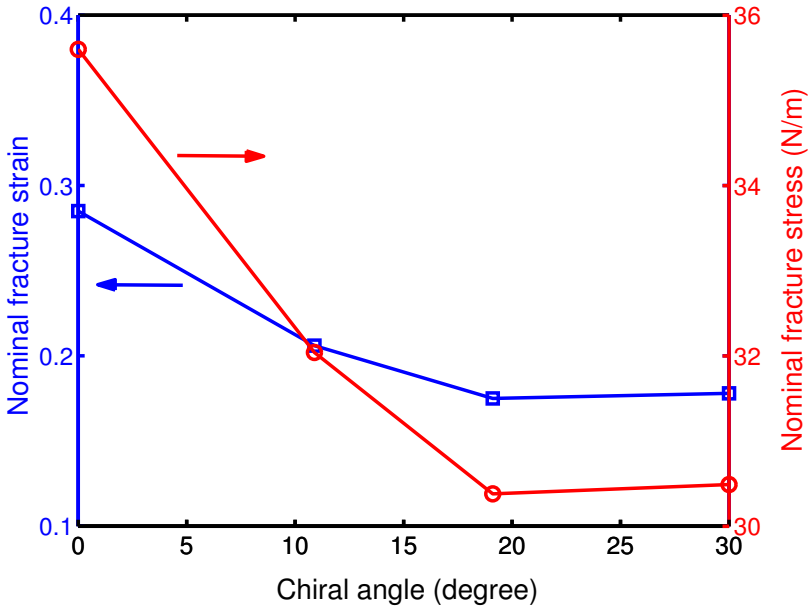

Fracture occurs as a result of intrinsic instability of the homogeneous deformation:

$$\frac{\partial P}{\partial \varepsilon} = \frac{\partial^2 \Phi}{\partial \varepsilon^2} = 0$$

- The nominal stress and strain to fracture depend on the direction of uniaxial stretch.

Lu and Huang, Int. J. Applied Mechanics 1, 443-467 (2009).

Monolayer graphene under uniaxial tension

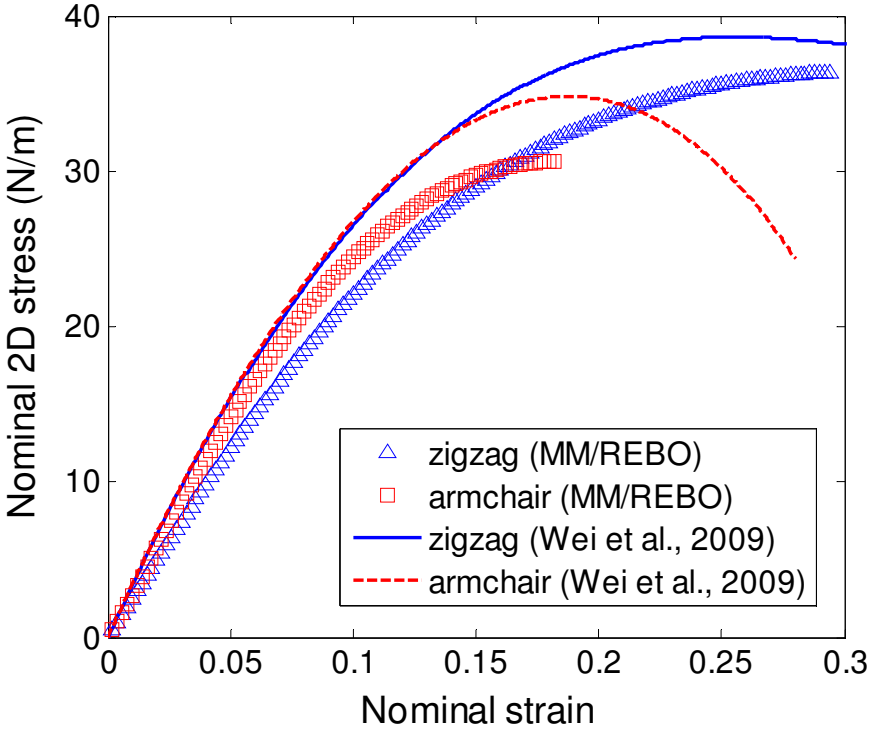

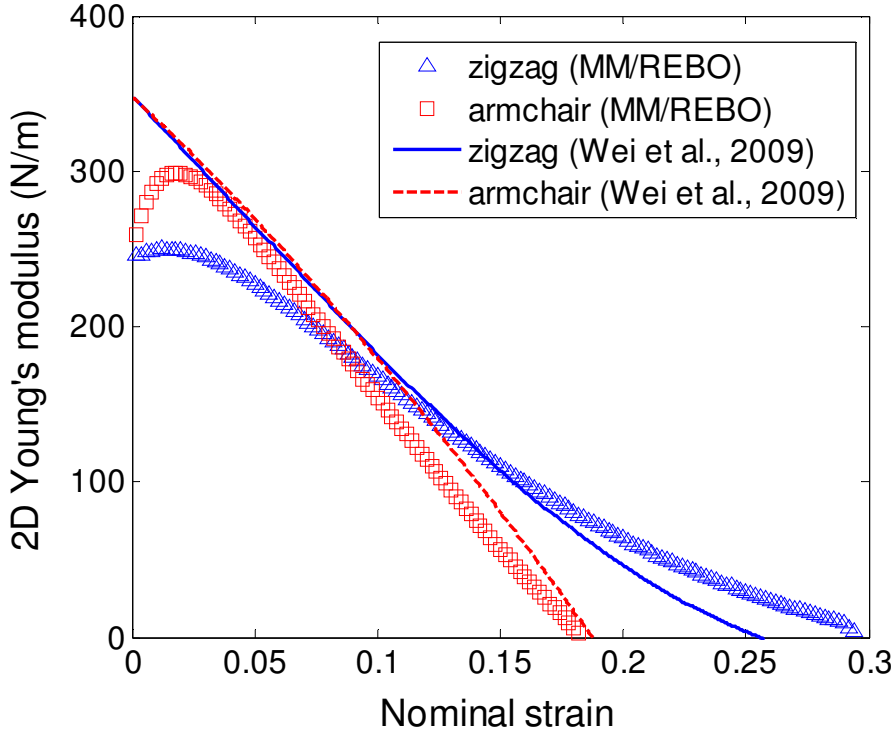

- **Disagreement:** the REBO potential underestimates the initial Young's modulus.
- **Agreement:** the fracture stress/strain is higher in the zigzag direction than in the armchair direction.

Bending Modulus of Monolayer Graphene

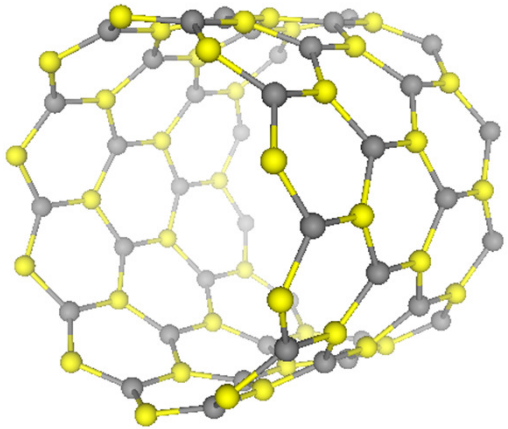

- Bending moment-curvature is nearly linear, with slight anisotropy.
- Including the dihedral angle effect leads to higher bending energy and bending modulus.

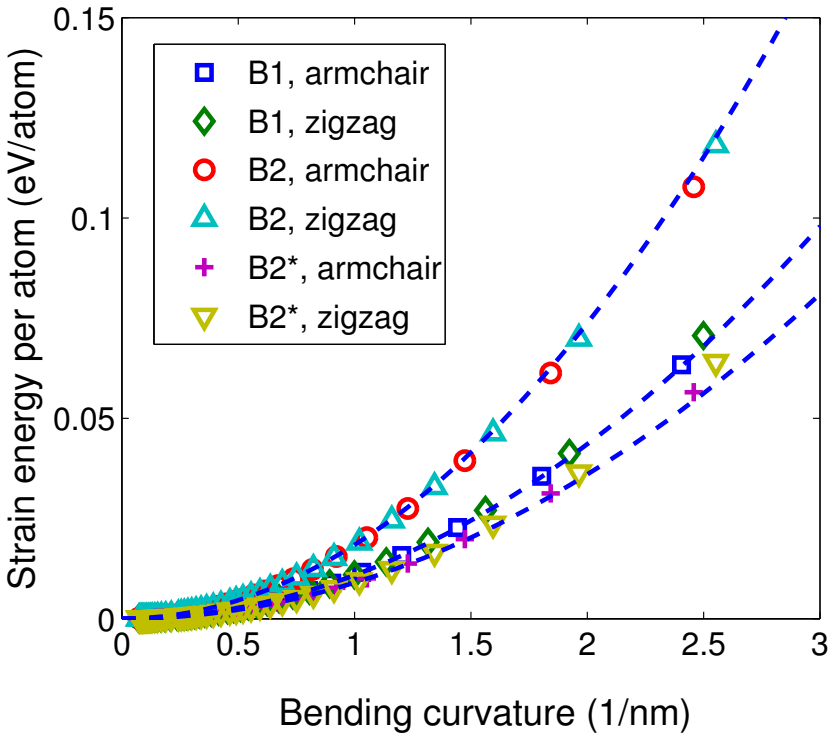

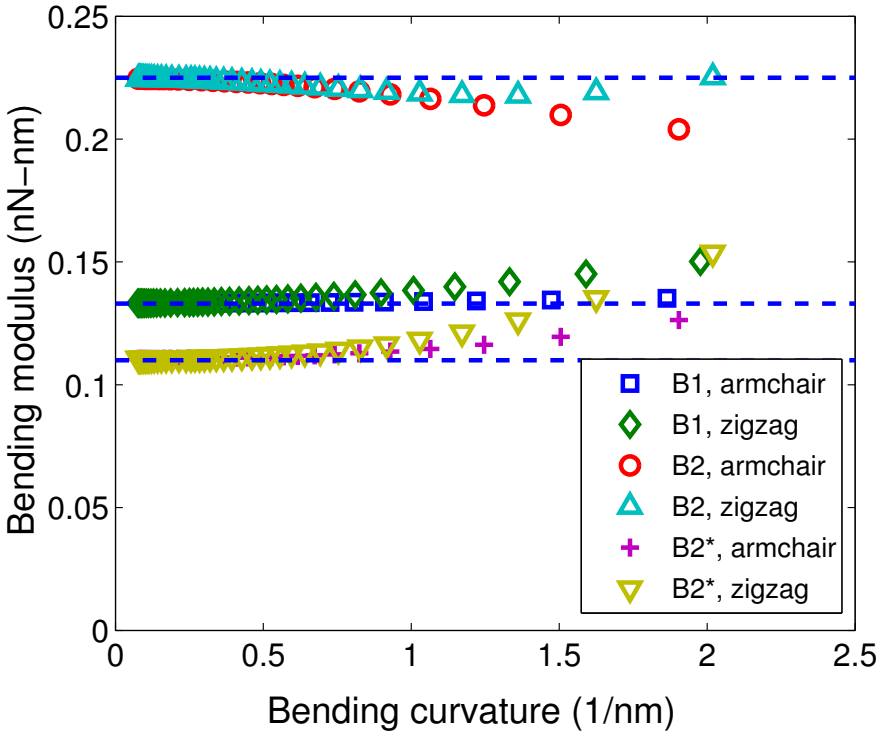

Lu, Arroyo, and Huang, J. Phys. D: Appl. Phys. 42, 102002 (2009).

Effect of dihedral angle

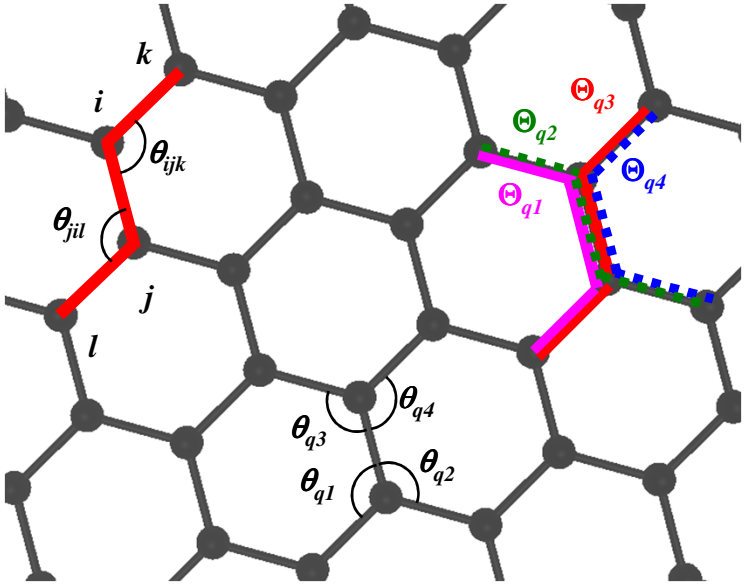

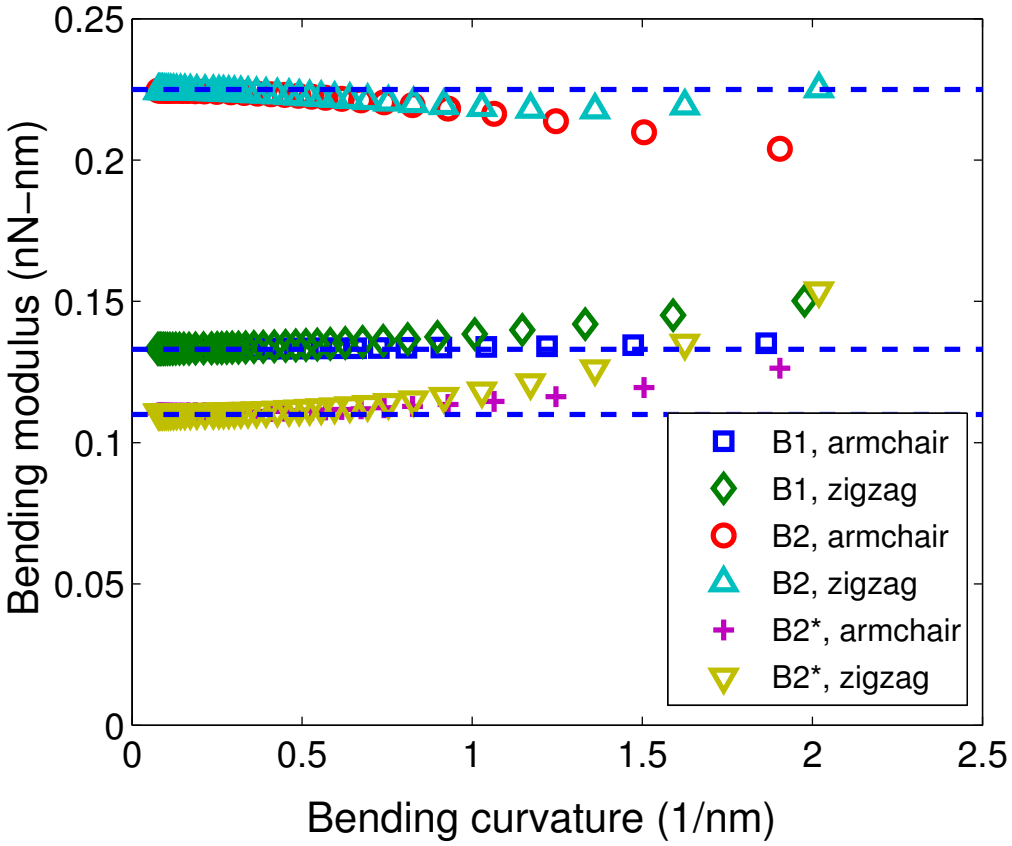

$$V_{ij} = V_R(r_{ij}) - \bar{b}_{ij} V_A(r_{ij})$$

$$\bar{b}_{ij} = \tfrac{1}{2}\left(b_{ij}^{\sigma-\pi} + b_{ji}^{\sigma-\pi}\right) + b_{ij}^{DH} + \Pi_{ij}^{RC}$$

$$b_{ij}^{DH} = \frac{T_0}{2} \sum_{k,l(\neq i,j)} \left[\left(1 - \cos^2 \Theta_{ijkl}\right) f_c(r_{ik}) f_c(r_{jl})\right]$$

$$\cos\Theta_{ijkl} = \mathbf{n}_{jik} \cdot \mathbf{n}_{ijl}$$

Lu, Arroyo, and Huang, J. Phys. D: Appl. Phys. 42, 102002 (2009).

Physical Origin of Bending Modulus

Bending modulus of a thin elastic plate:

$$D = \frac{dM}{d\kappa} \sim Eh^3$$

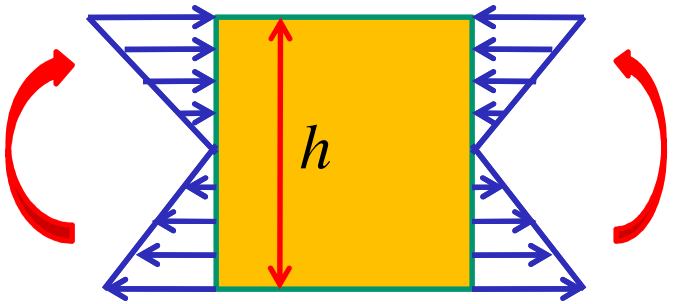

For monolayer graphene, bending moment and bending stiffness result from multibody interatomic interactions (second and third nearest neighbors).

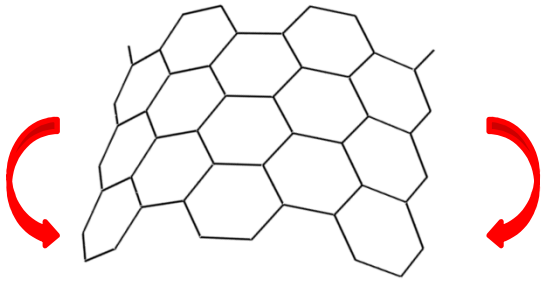

$$D = \frac{V_A(r_0)}{2}\left(\frac{\partial b_{ij}^{\sigma-\pi}}{\partial \theta_{ijk}} - \frac{14T_0}{\sqrt{3}}\right)$$

- D = 0.83 eV (0.133 nN-nm) by REBO-1
- D = 1.4 eV (0.225 nN-nm) by REBO-2
- D = 1.5 eV (0.238 nN-nm) by first principle

Lu, Arroyo, and Huang, J. Phys. D: Appl. Phys. 42, 102002 (2009).

Coupling between bending and stretching

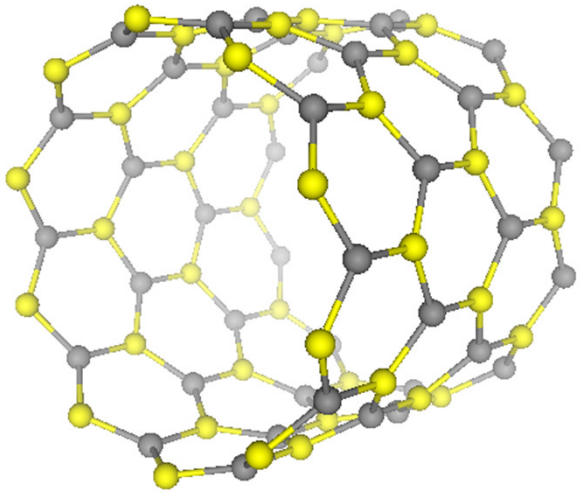

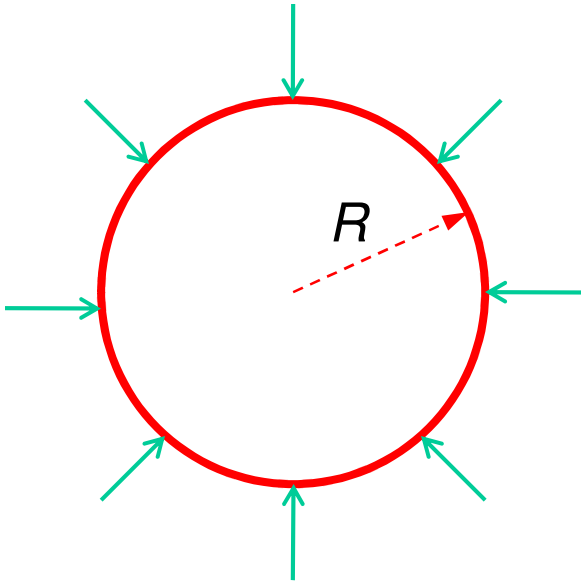

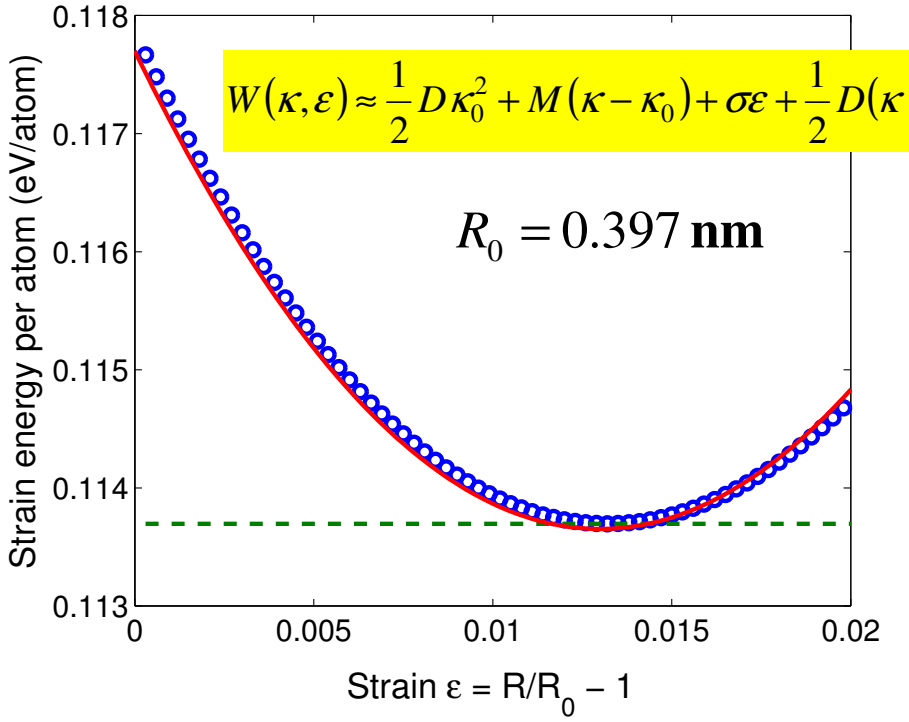

- The tube radius increases upon relaxation, leading to simultaneous bending and stretching.

Lu, Arroyo, and Huang, J. Phys. D: Appl. Phys. 42, 102002 (2009).

Excess Edge Energy and Edge Force

Zigzag edge:

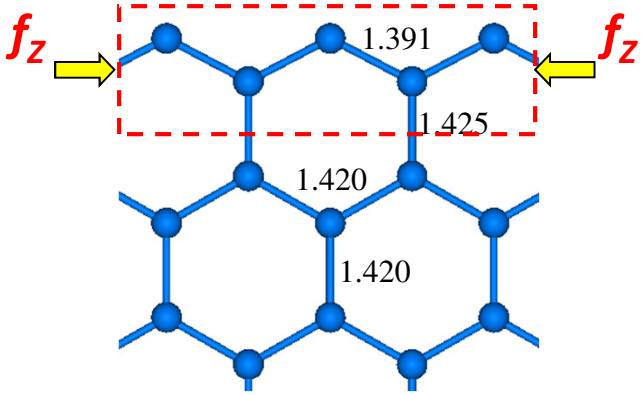

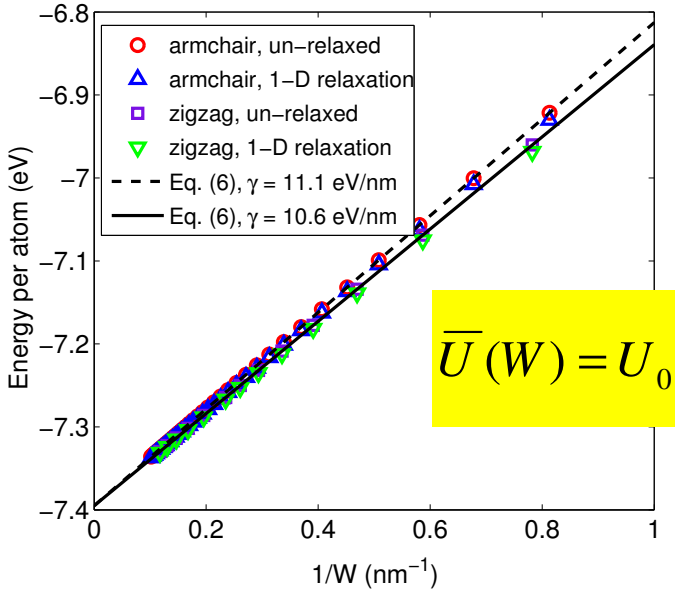

$$\overline{U}(W) = U_0 + \frac{2\gamma}{N} = U_0 + \frac{S_0}{W}\gamma$$

Armchair edge:

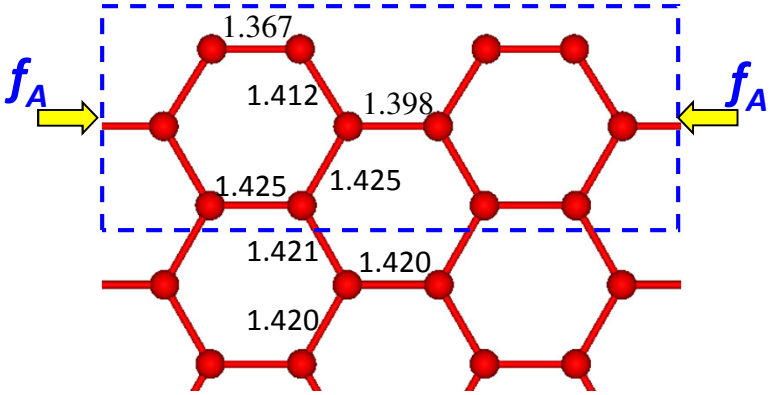

	Edge energy (eV/nm)		Edge force (eV/nm)		r_0
	Armchair	Zigzag	Armchair	Zigzag	(nm)
DFT [17] (GPAW)	9.8	13.2	-	-	0.142
DFT [18] (VASP)	10	12	-14.5	-5	0.142
DFT [22] (SIESTA)	12.43	15.33	-26.40	-22.48	0.142
MM [20] (AIREBO)	-	-	-10.5	-20.5	0.140
MD [21]	-	-	-20.4	-16.4	0.146
MM (REBO)	10.91	10.41	-8.53	-16.22	0.142

Lu and Huang, Phys. Rev. B 81, 155410 (2010).

Edge buckling of GNRs

Zigzag GNR

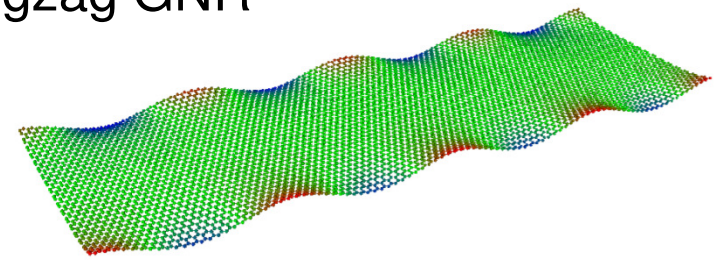

Intrinsic wavelength ~ 6.2 nm

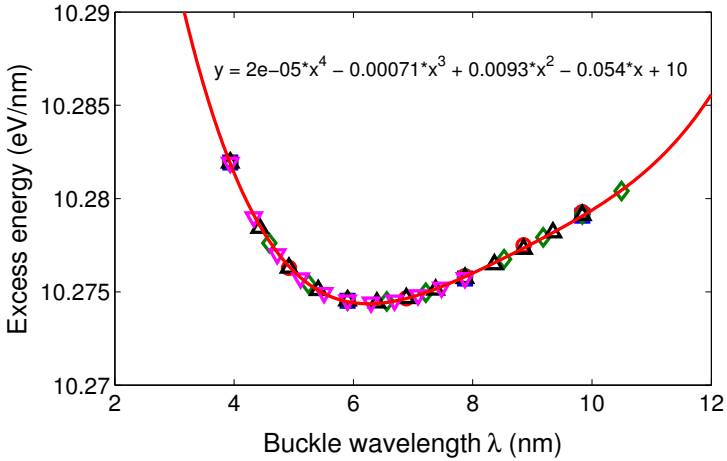

Armchair GNR

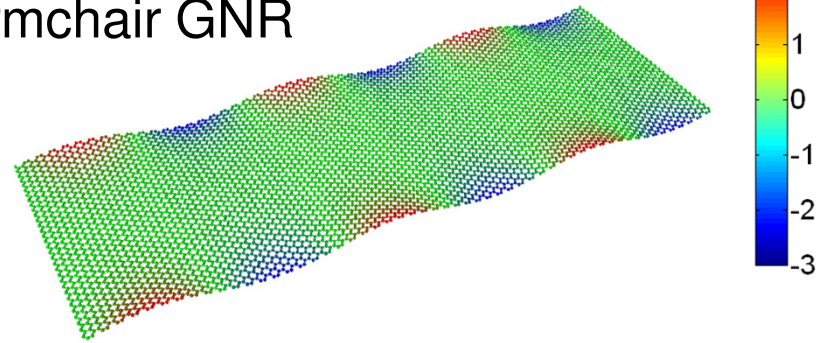

Intrinsic wavelength ~ 8.0 nm

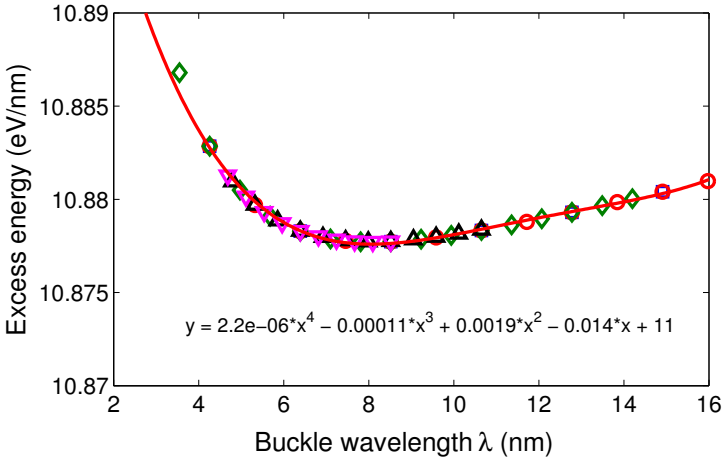

➢ The wavelengths for edge buckling do not scale with *D*/*f*.

Lu and Huang, Phys. Rev. B 81, 155410 (2010).

GNRs under Uniaxial Tension

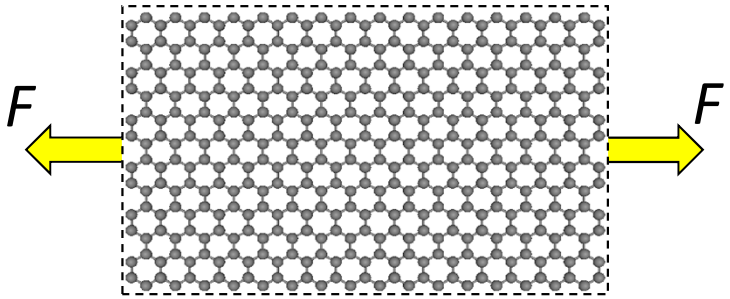

$$U(\varepsilon) = \Phi(\varepsilon) WL + 2\gamma(\varepsilon) L$$

$$\delta U = FL\delta\varepsilon$$

$$\sigma = \frac{F}{W} = \frac{1}{WL}\frac{dU}{d\varepsilon} = \frac{d\Phi}{d\varepsilon} + \frac{2}{W}\frac{d\gamma}{d\varepsilon}$$

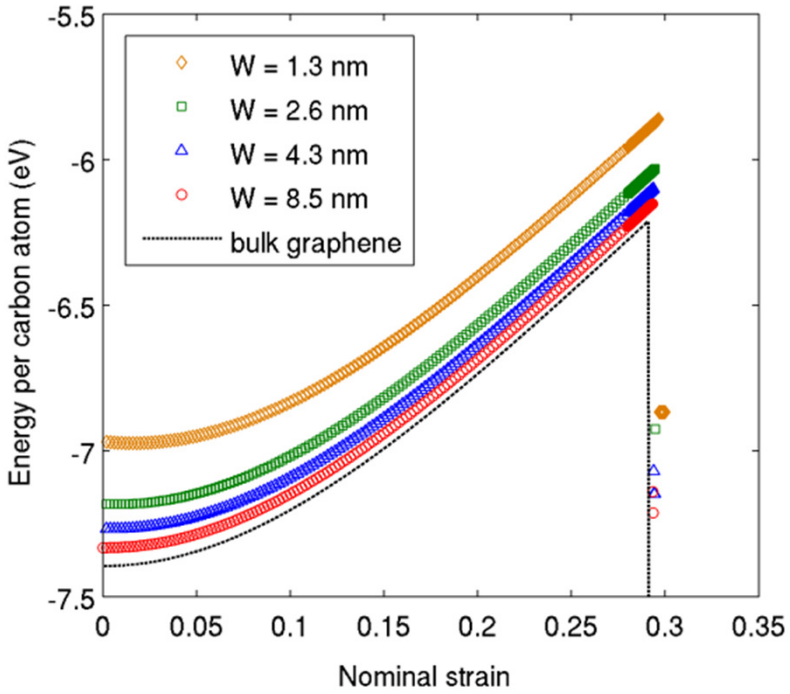

Zigzag GNRs

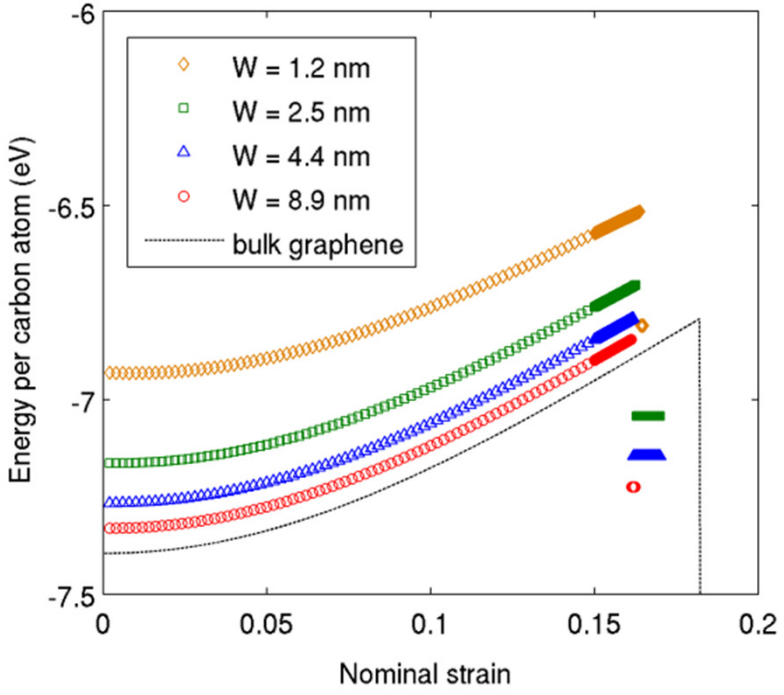

Armchair GNRs

GNRs under Uniaxial Tension

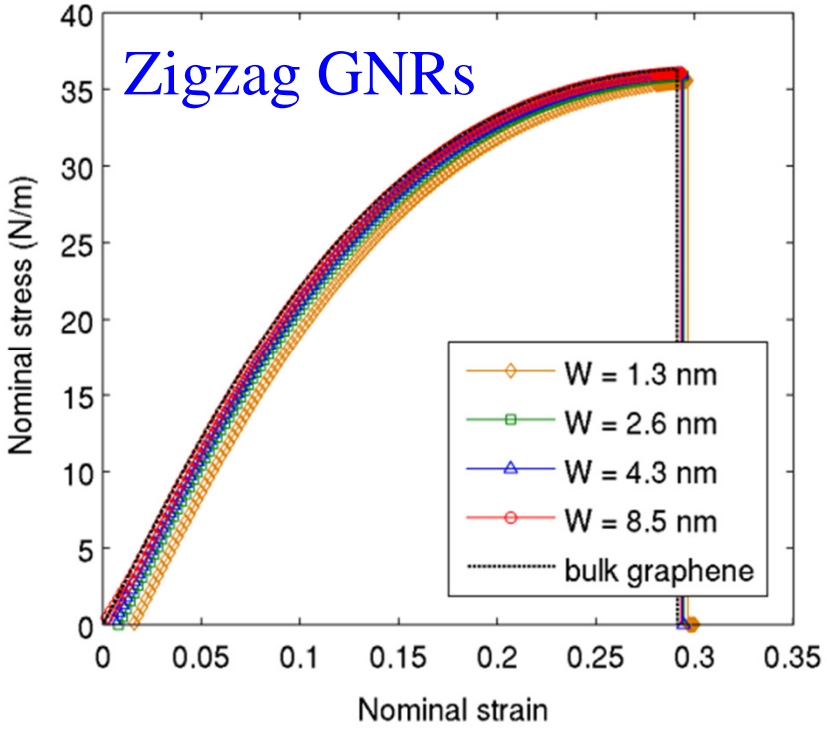

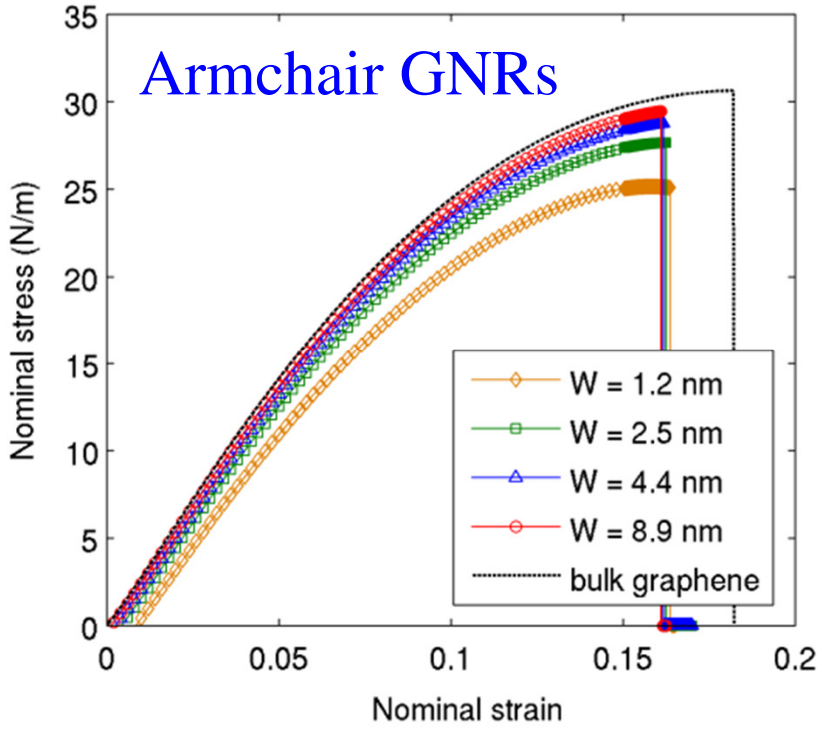

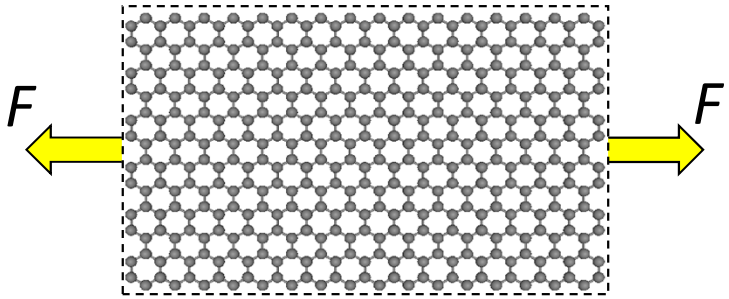

$$\sigma(\varepsilon) = \frac{F}{W} = \frac{d\Phi}{d\varepsilon} + \frac{2}{W}\frac{d\gamma}{d\varepsilon}$$

Lu and Huang, arXiv:1007.3298 (2010).

2D Young's Moduli of GNRs

$$\sigma(\varepsilon) = \frac{d\Phi}{d\varepsilon} + \frac{2}{W}\frac{d\gamma}{d\varepsilon}$$

$$E(\varepsilon) = \frac{d^2\Phi}{d\varepsilon^2} + \frac{2}{W}\frac{d^2\gamma}{d\varepsilon^2}$$

Young's modulus under infinitesimal strain:

$$E_0 = E_0^{bulk} + \frac{2}{W}E_0^{edge}$$

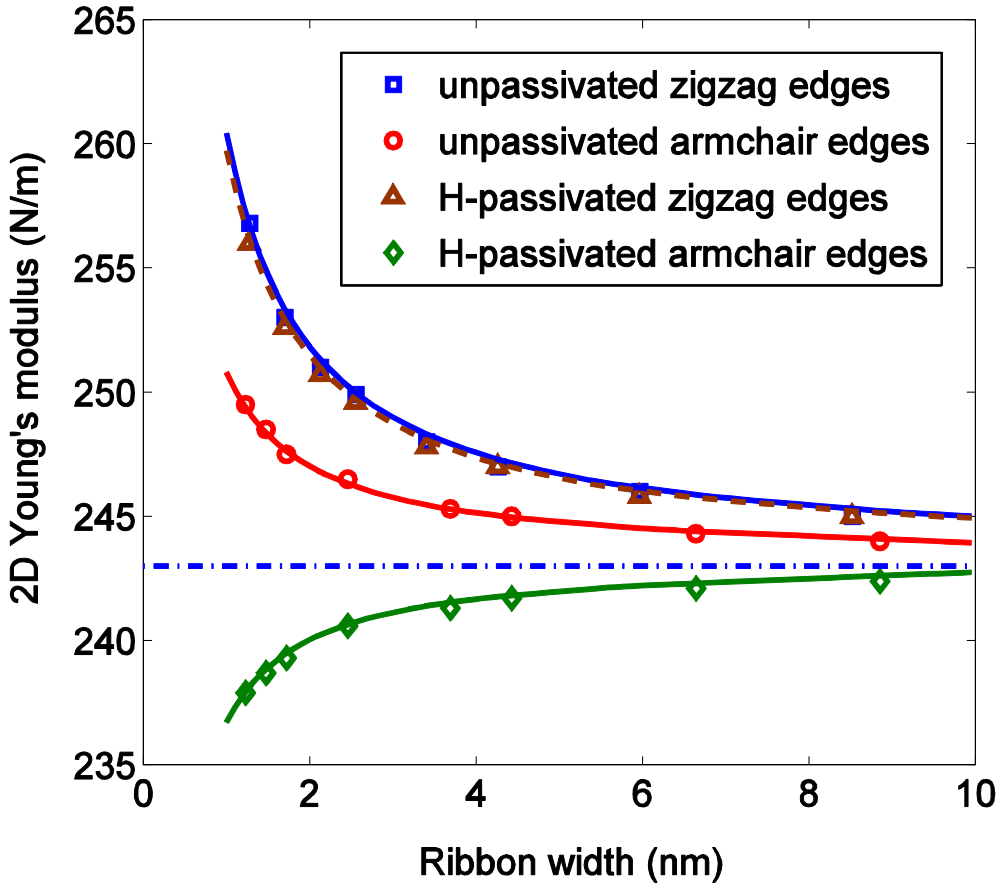

The nonlinear dependence of the excess edge energy on strain leads to anisotropic, width-dependent Young's modulus for GNRs.

Lu and Huang, arXiv:1007.3298 (2010).

Fracture of graphene nanoribbons

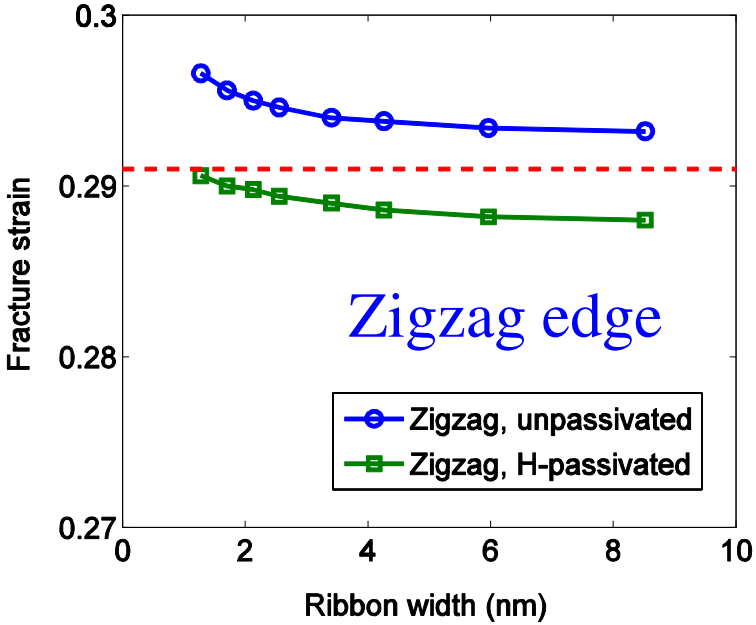

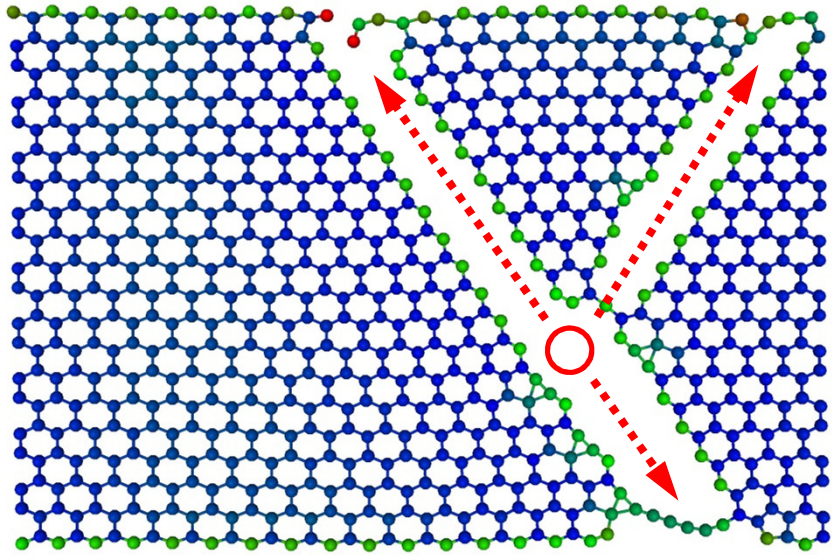

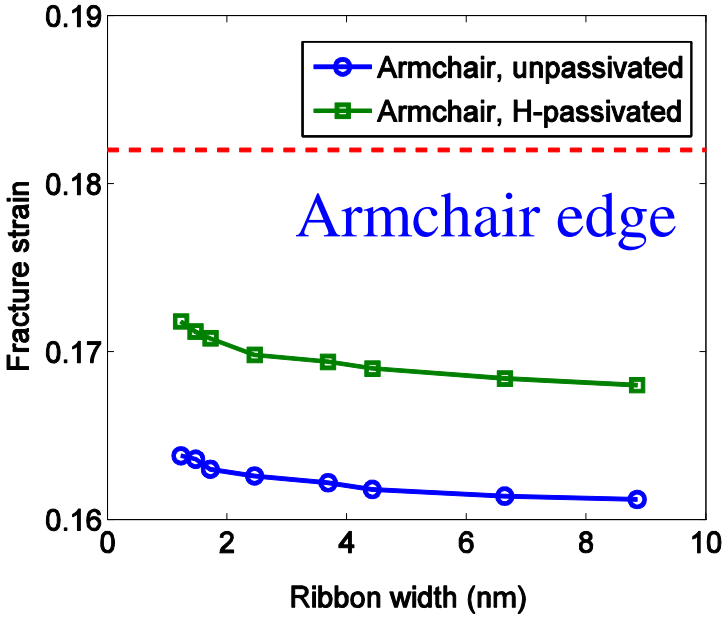

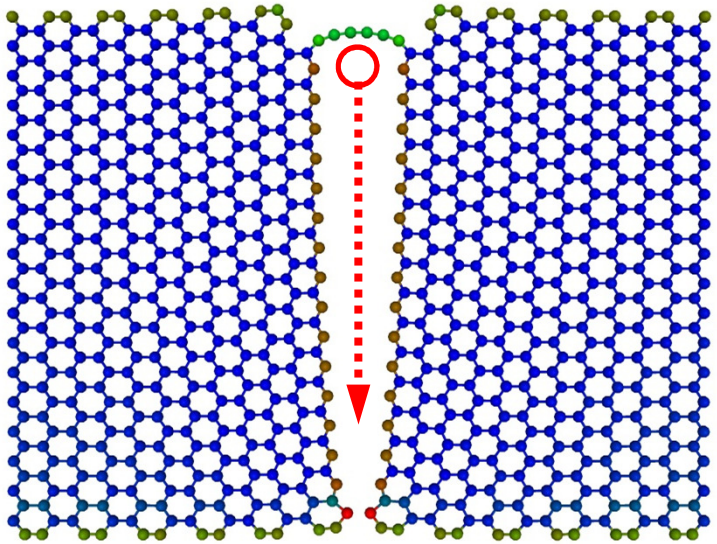

Lu and Huang, arXiv:1007.3298 (2010).

Graphene on Oxide Substrates

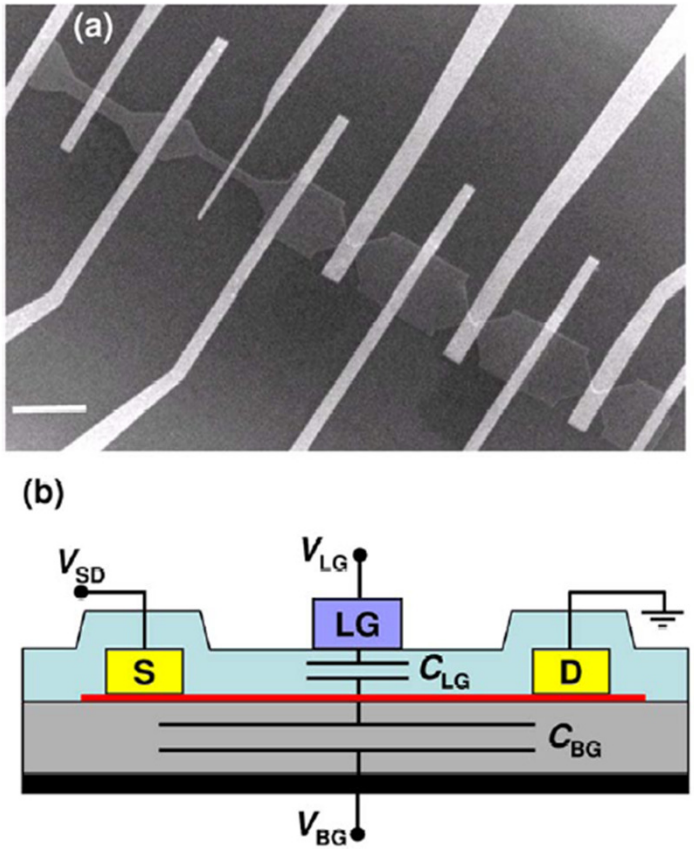

Ozyilmaz et al., 2007.

HR-STM image (Stolyarova et al., 2007)

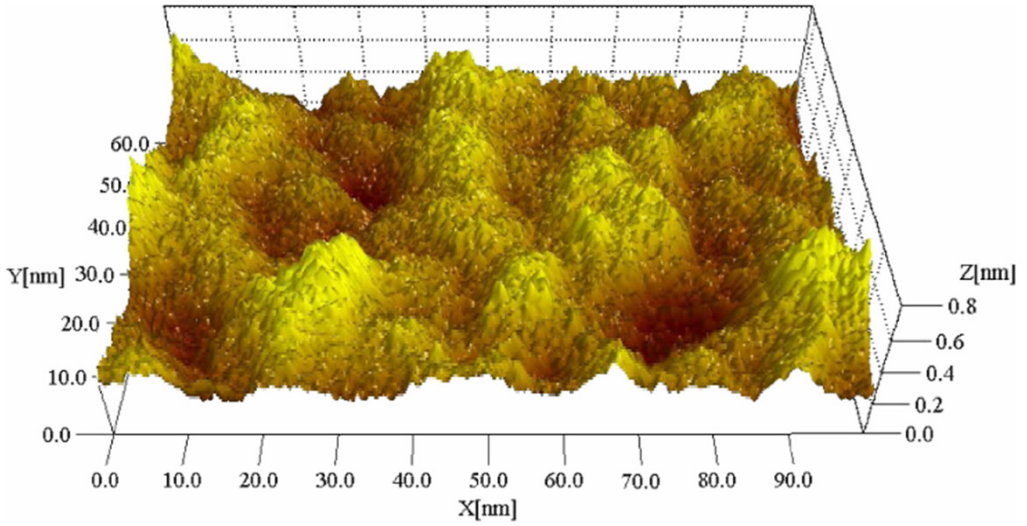

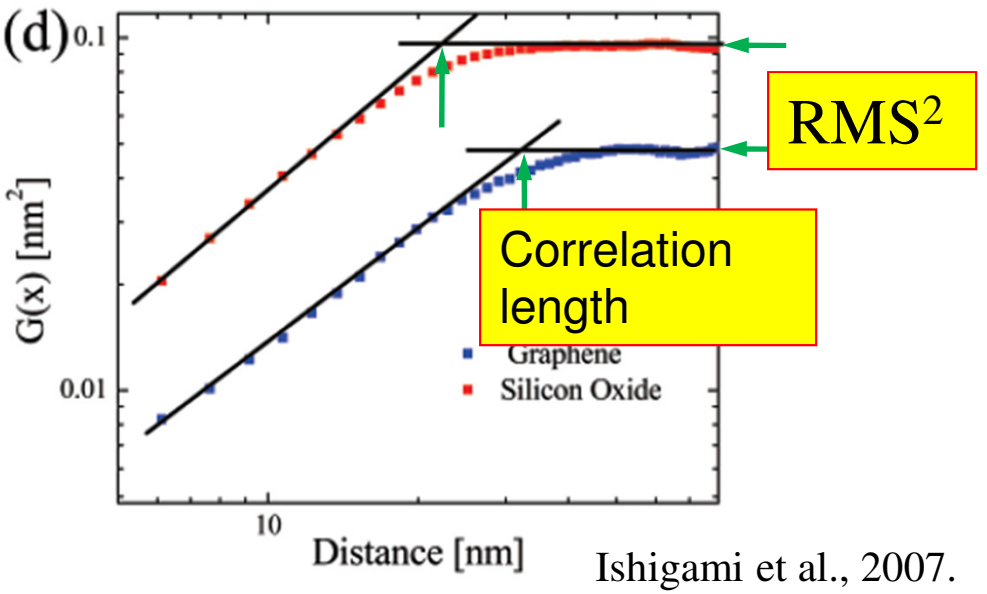

Ishigami et al., 2007.

The 3D morphology is important for the transport properties of graphene-based devices.

Van der Waals Interaction

Lennard-Jones potential for particle-particle interactions:

$$W_{LJ}(r) = -\frac{C_1}{r^6} + \frac{C_2}{r^{12}}$$

Monolayer-substrate interaction (energy per unit area):

$$U(h) = -\Gamma_0 \left[\frac{3}{2}\left(\frac{h_0}{h}\right)^3 - \frac{1}{2}\left(\frac{h_0}{h}\right)^9 \right]$$

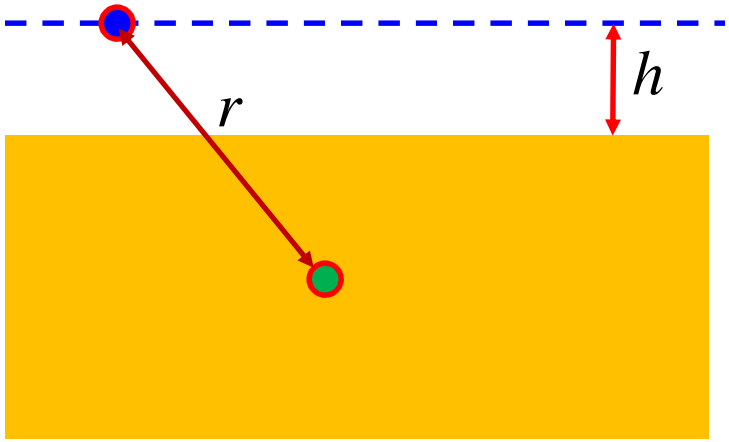

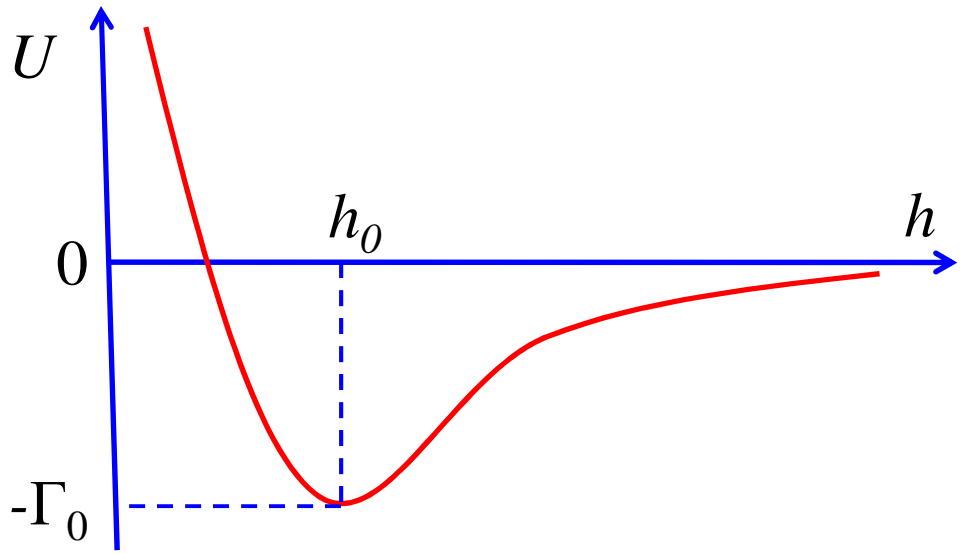

Aitken and Huang, J. Appl. Phys. 107, 123531 (2010).

Van der Waals Thickness and Energy

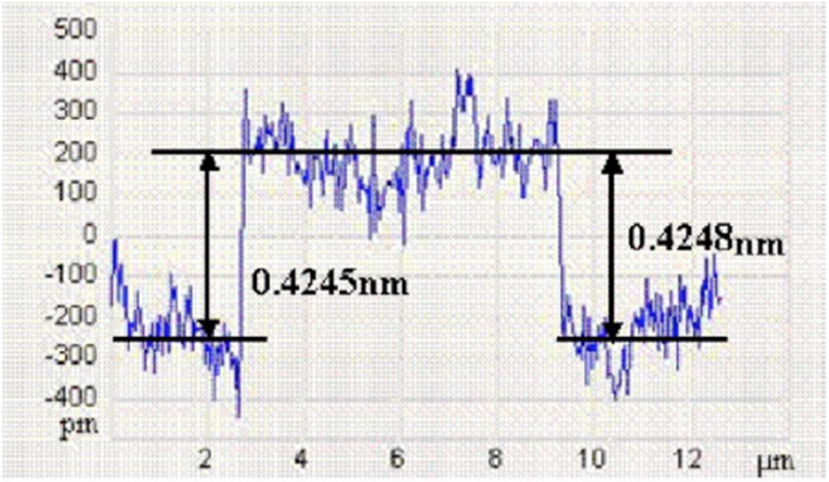

Sonde et al., 2009.

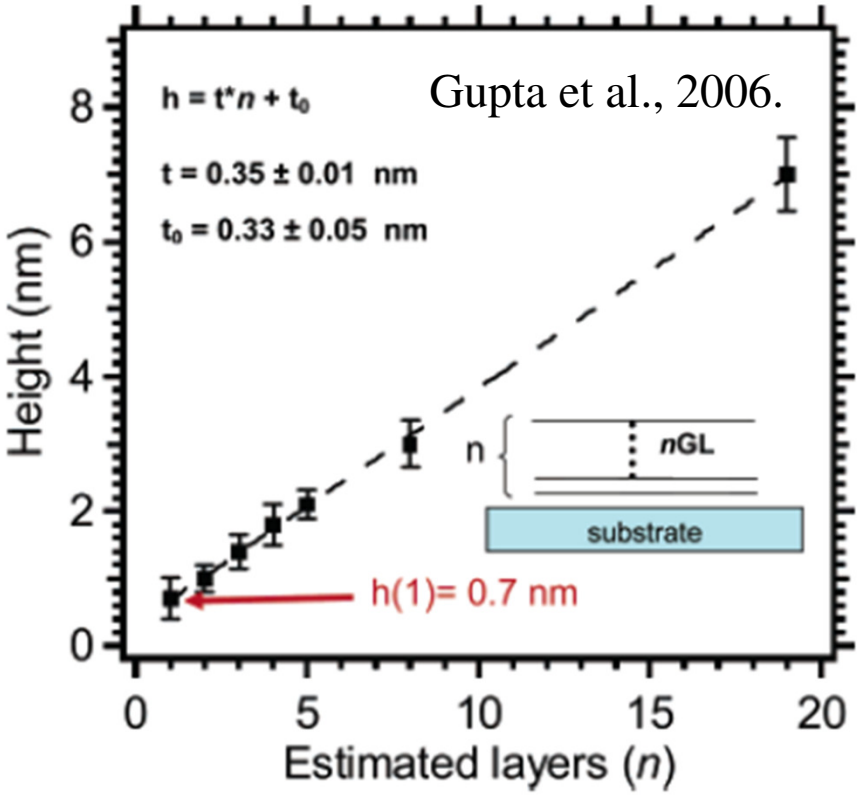

- Interlayer spacing in graphite ~ **0.34 nm**;
- AFM measurements of h_0 for graphene on oxide range from **0.4 to 0.9 nm**;
- The adhesion energy (Γ_0) has not been measured directly;
- Theoretically estimated values for Γ_0 range from **0.6 to 0.8 eV/nm^2**.

Flat Graphene on Flat Surface

Interfacial strength: $\sigma_{\max} = 1.466\frac{\Gamma_0}{h_0}$

Initial stiffness: $k_0 = \frac{27\Gamma_0}{h_0^2}$

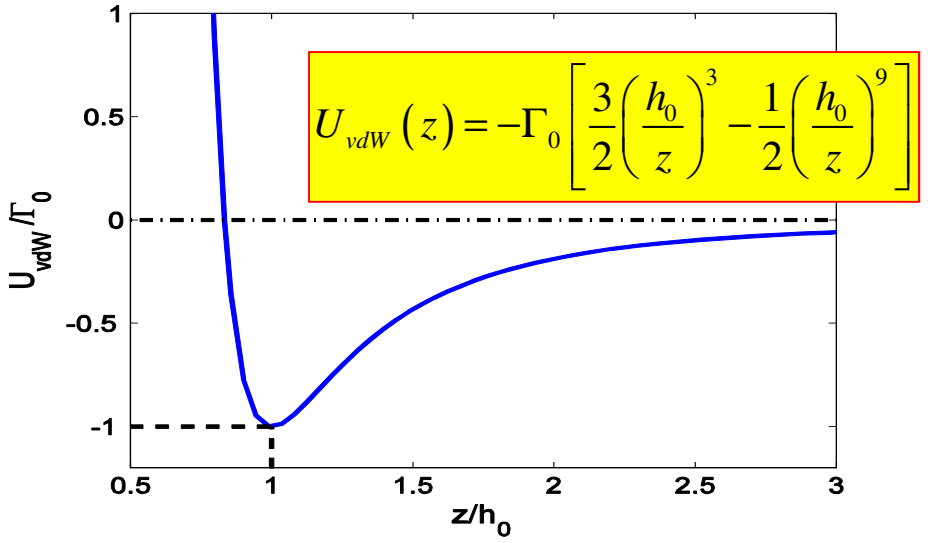

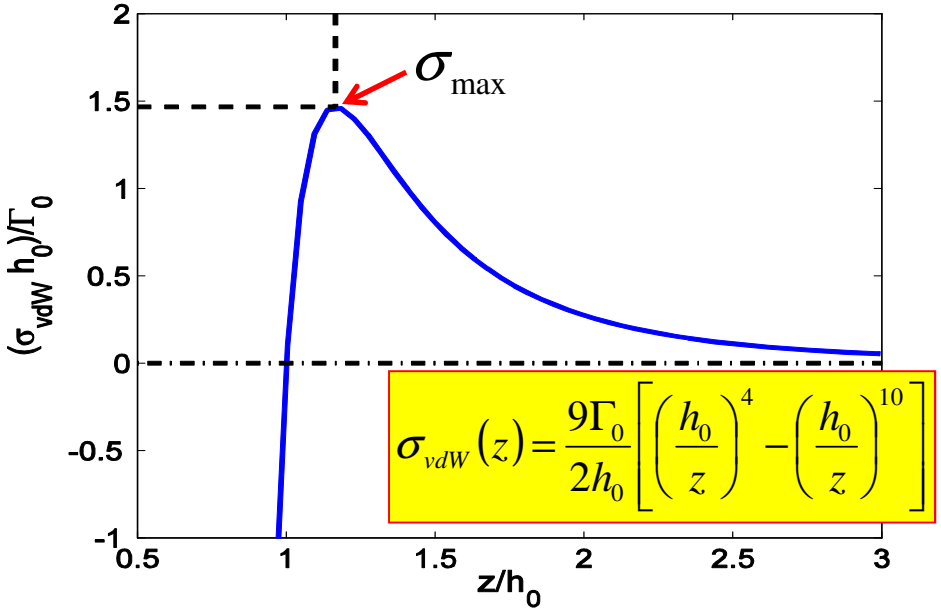

Representative values:

$h_0 = 0.6\,nm$ $\quad \Gamma_0 = 0.6\,\mathbf{eV/nm^2}$

$\sigma_{\max} = 230\,MPa$ $\quad k_0 = 7200\,\mathbf{MPa/nm}$

Aitken and Huang, J. Appl. Phys. 107, 123531 (2010).

Strain-Induced Instability

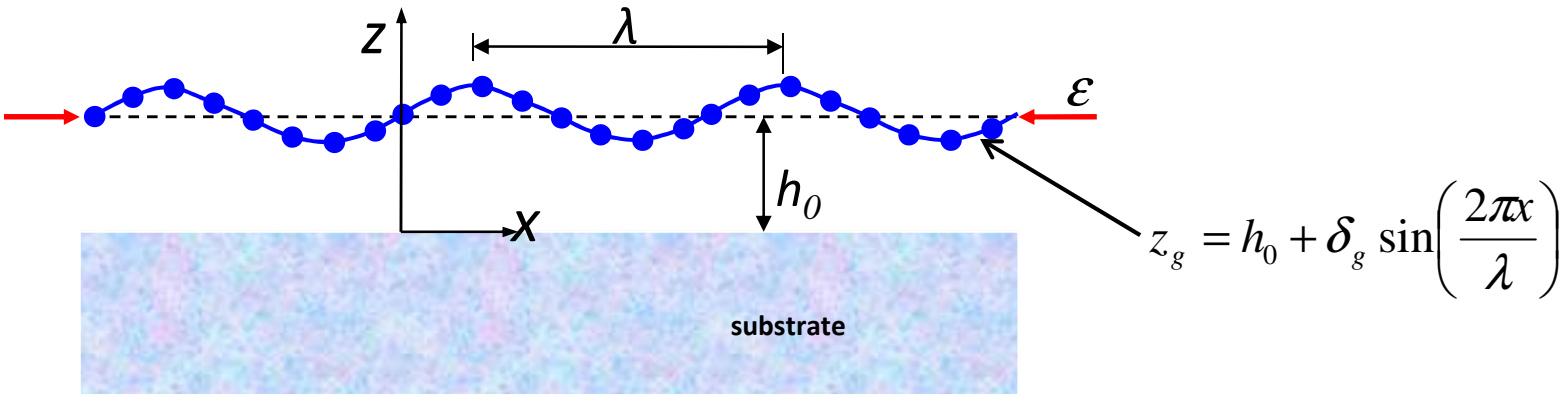

- The competition between the elastic strain energy of graphene and the van der Waals interaction energy sets a critical strain for instability as well as the equilibrium corrugation wavelength beyond the critical strain.

Elastic strain energy of graphene:

$$\tilde{U}_g \approx \left[\underbrace{\frac{C\varepsilon}{4}\left(\frac{2\pi}{\lambda}\right)^2}_{In-Plane} + \underbrace{\frac{D}{4}\left(\frac{2\pi}{\lambda}\right)^4}_{Bending}\right]\delta_g^2 + \underbrace{\frac{3C}{64}\left(\frac{2\pi}{\lambda}\right)^4}_{In-Plane}\delta_g^4$$

Van der Waals Interaction Energy:

$$\tilde{U}_{vdW} \approx \Gamma_0\left(-1 + \frac{27}{4}\left(\frac{\delta_g}{h_0}\right)^2 + \frac{675}{8}\left(\frac{\delta_g}{h_0}\right)^4\right)$$

Total free energy:

$$\tilde{U} = \tilde{U}_g + \tilde{U}_{vdW}$$

Aitken and Huang, J. Appl. Phys. 107, 123531 (2010).

Strain-Induced Corrugation of Graphene

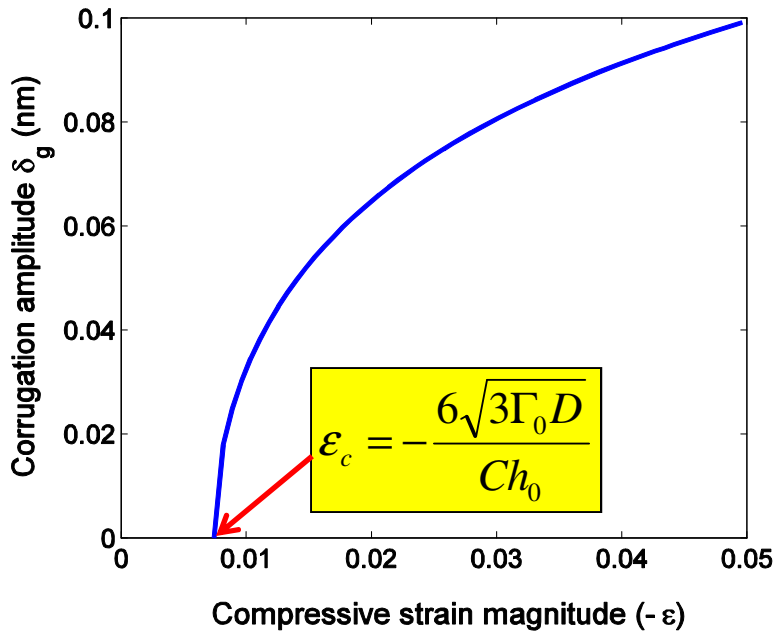

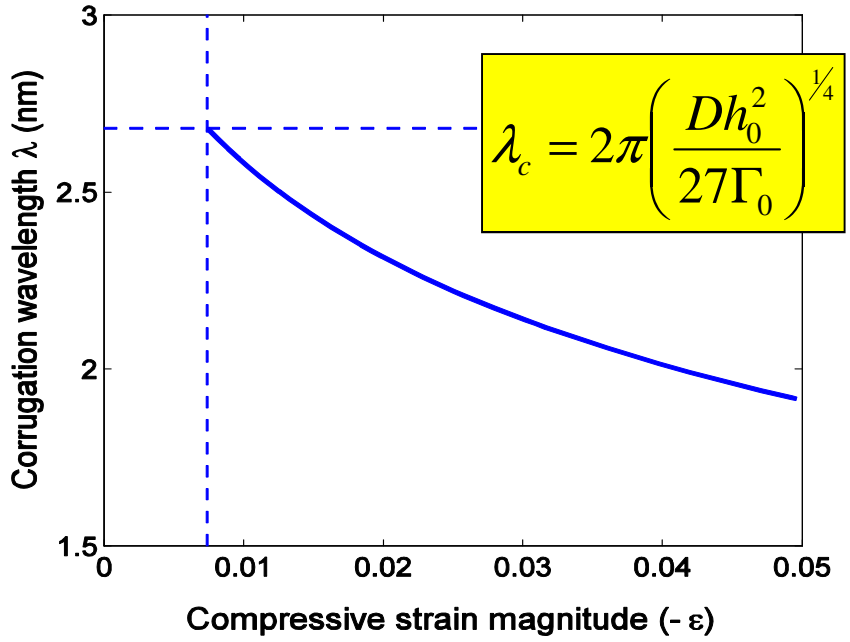

- On a flat surface, a graphene monolayer is flat and stable below a critical compressive strain;
- Beyond the critical strain, the monolayer corrugates with increasing amplitude and decreasing wavelength.

Representative values:

$h_0 = 0.6\,nm$ $\quad \Gamma_0 = 0.6\,\mathbf{eV/nm^2}$

$C = 353\,\mathbf{N/m}$ $\quad D = 1.5\,\mathbf{eV}$

$\varepsilon_c = -0.0074$

$\lambda_c = 2.68\,nm$

Aitken and Huang, J. Appl. Phys. 107, 123531 (2010).

Graphene on a Corrugated Surface

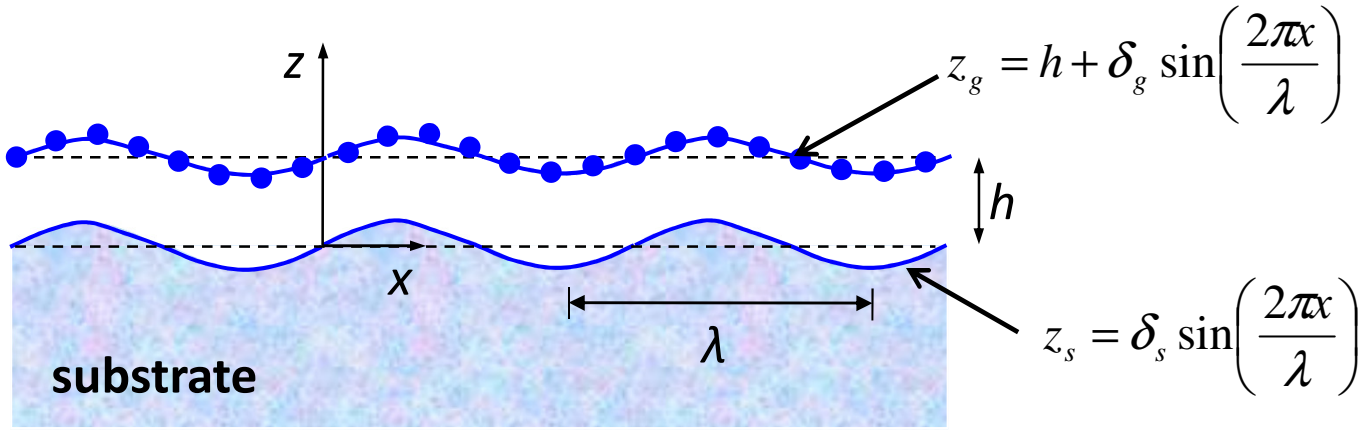

van der Waals interaction energy:

$$\tilde{\tilde{U}}_{vdW}(h,\delta_g) \approx U_{vdW}(h) + U_1(h)\left[\left(\frac{\delta_g}{h_0}\right)^2 + \left(\frac{\delta_s}{h_0}\right)^2\right] + U_2(h)\frac{\delta_g \delta_s}{h_0^2}$$

$$U_1(h) = \frac{9\Gamma_0}{2}\left[-\left(\frac{h_0}{h}\right)^5 + \frac{5}{2}\left(\frac{h_0}{h}\right)^{11}\right] = \frac{h_0^2}{4}k_{vdW}(h)$$

$$U_2(h) = 9\pi^3\Gamma_0\left[\frac{h_0^5}{\lambda^3 h^2}K_3\left(\frac{2\pi h}{\lambda}\right) - \frac{\pi^3 h_0^{11}}{24\lambda^6 h^5}K_6\left(\frac{2\pi h}{\lambda}\right)\right]$$

Total free energy:

$$\tilde{\tilde{U}} = \tilde{U}_g + \tilde{\tilde{U}}_{vdW}$$

Given δ_s and λ, minimize the total energy to find δ_g and h

Aitken and Huang, J. Appl. Phys. 107, 123531 (2010).

Substrate Induced Corrugation of Graphene

$$\frac{\delta_g}{\delta_s} = f\left(\frac{\lambda}{h_0}, \frac{\delta_s}{h_0}; \frac{D}{\Gamma_0 h_0^2}, \frac{C\varepsilon}{\Gamma_0}\right)$$

$$\frac{h}{h_0} = g\left(\frac{\lambda}{h_0}, \frac{\delta_s}{h_0}; \frac{D}{\Gamma_0 h_0^2}, \frac{C\varepsilon}{\Gamma_0}\right)$$

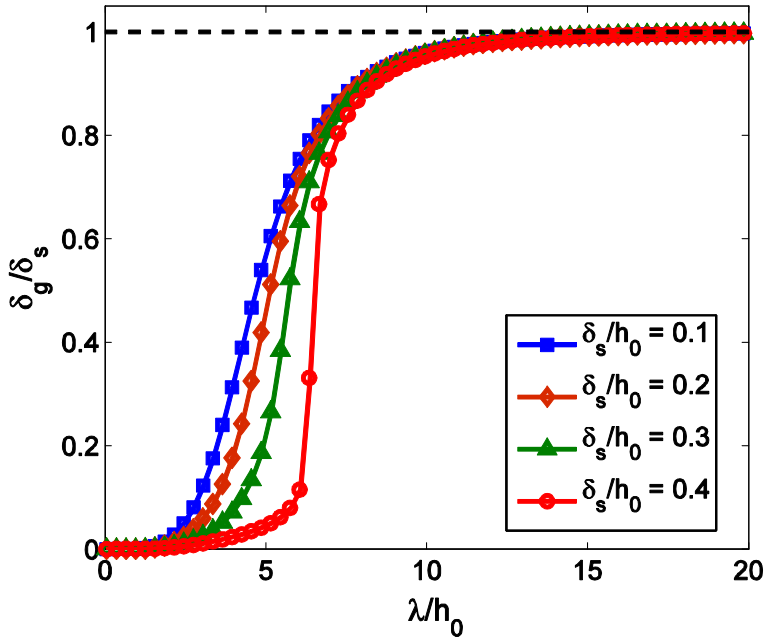

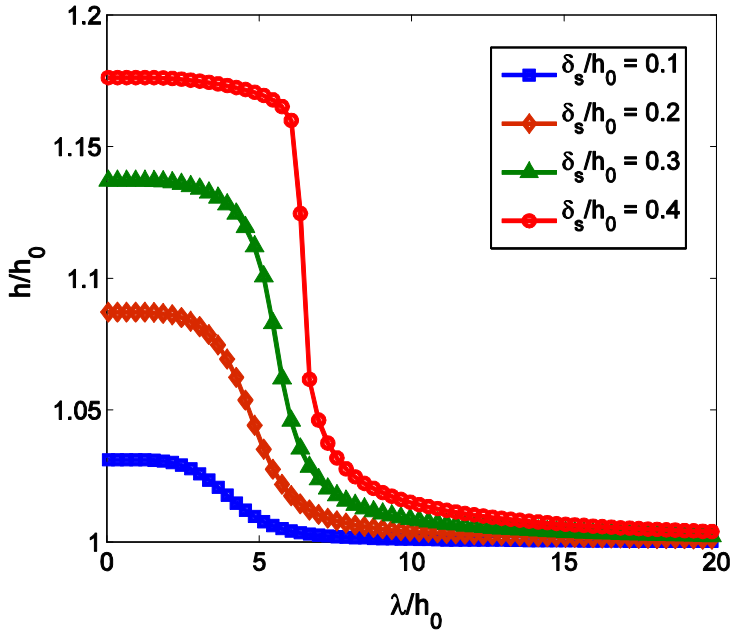

- ***Conformal*** at ***long*** wavelengths.
- ***Non-conformal*** at ***short*** wavelengths.
- Transition between the two states depends on the amplitude of substrate surface corrugation, becoming more abrupt with increasing amplitude.

Aitken and Huang, J. Appl. Phys. 107, 123531 (2010).

Effect on Adhesion Energy

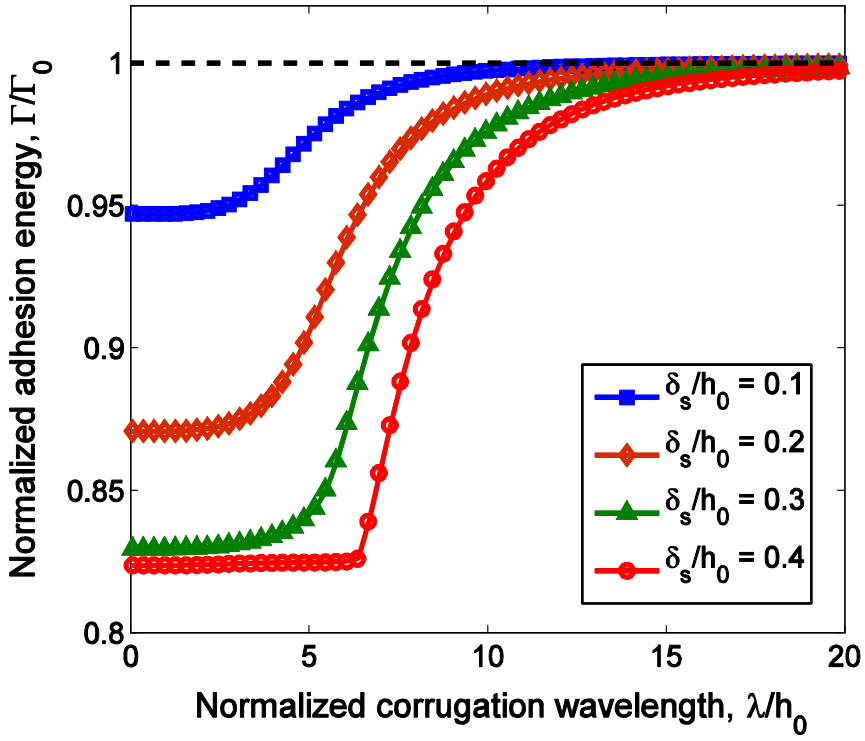

- The adhesion energy decreases as the corrugation wavelength decreases, approaching a plateau at the short-wavelength limit.
- The adhesion energy decreases with increasing amplitude of the substrate surface corrugation.
- Better adhesion at the conformal state than the non-conformal state.

Aitken and Huang, J. Appl. Phys. 107, 123531 (2010).

Effects of Mismatch Strain

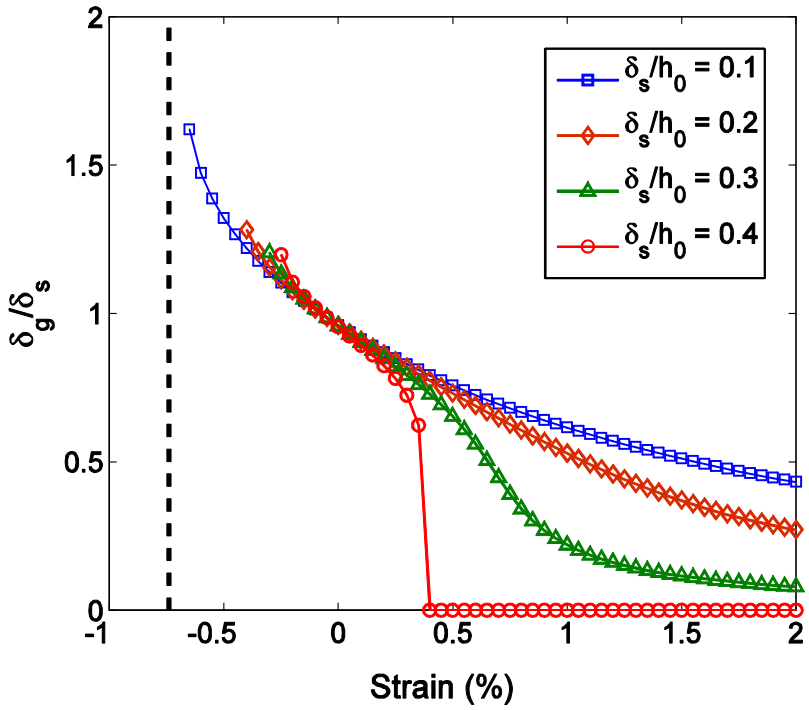

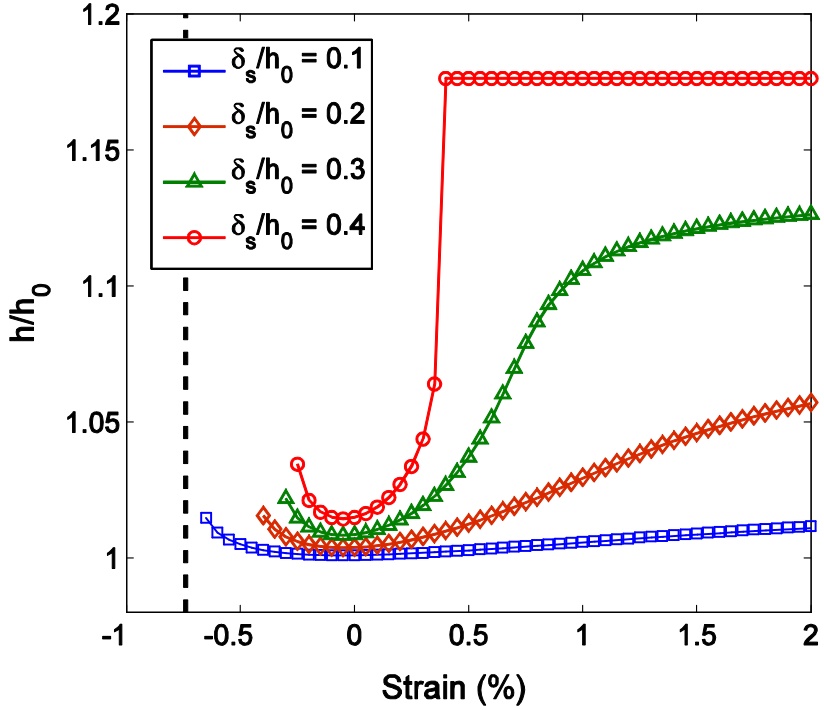

- A tensile strain tends to flatten the supported graphene, while a compressive strain tends to increase the corrugation amplitude.
- A "snap-through" instability occurs at a critical tensile strain.
- A "buckling" instability occurs at a critical compressive strain.

Aitken and Huang, J. Appl. Phys. 107, 123531 (2010).

Critical Strain for Buckling Instability

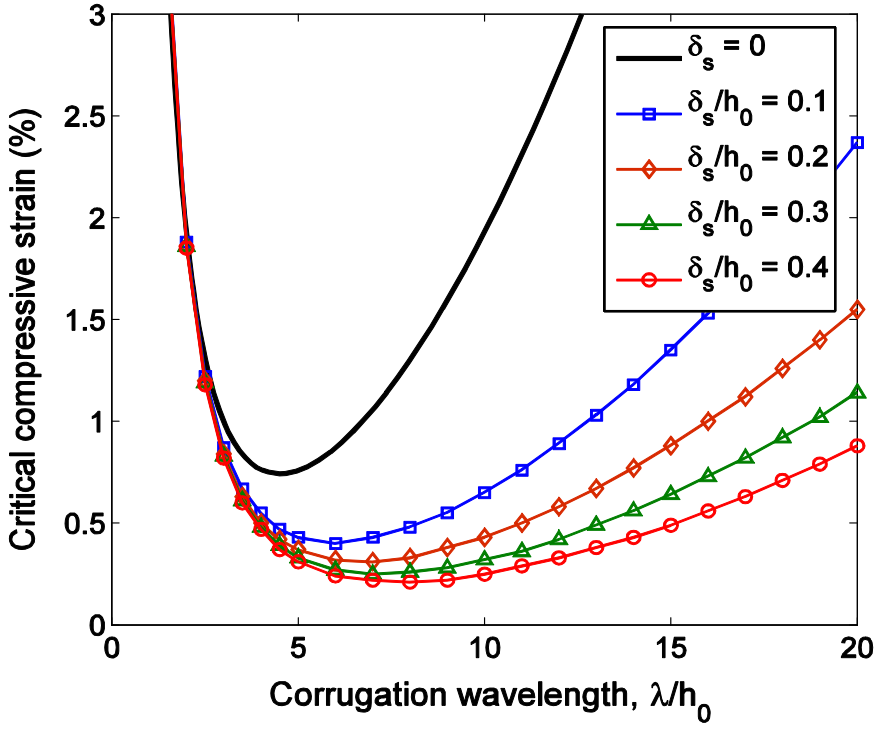

- With increasing amplitude of the substrate surface corrugation:
  - The critical compressive strain for buckling decreases.
  - The corresponding buckling wavelength increases.

Aitken and Huang, J. Appl. Phys. 107, 123531 (2010).

Summary

- Nonlinear continuum mechanics for 2D graphene monolayer
- Atomistic modeling of graphene under bending and stretching
- Excess edge energy, edge forces, and induced edge buckling
- Graphene nanoribbons under uniaxial tension: edge effects on elastic modulus and fracture
- Graphene on oxide: van der Waals interaction and corrugation; strain-induced corrugation